Interactions of HCl and H2O with the surface of PuO2

DOI:
10.1016/j.jnucmat.2019.02.036

Document Version
Accepted author manuscript

Interactions of HCl and H_2O with the surface of PuO_2

Sophie Sutherland-Harper[1], Francis Livens[1], Carolyn Pearce[1,2], Jeff Hobbs[3], Robin Orr[4], Robin Taylor[4], Kevin Webb[4] and Nikolas Kaltsoyannis[1]

[1]School of Chemistry, University of Manchester, Oxford Road, Manchester, M13 9PL, UK; [2]Pacific Northwest National Laboratory, Richland, WA 99354, USA; [3]Sellafield Ltd., Sellafield, Seascale, Cumbria, CA20 1PG, UK; [4]National Nuclear Laboratory, Central Laboratory, Sellafield, Seascale, Cumbria, CA20 1PG, UK

Abstract

In order to explore the potential of heat treatment to decontaminate chloride-contaminated legacy plutonium dioxide (PuO_2) powders from the UK stockpile, samples retrieved from storage have been heated in air from 400 to 950 °C. These samples also contain high levels of other adsorbed gases from the atmosphere, including water. The amounts of chloride remaining on the PuO_2 particles after heat treatment (measured by a caustic leaching process) decrease whilst the amounts of volatilised chloride increase with increasing heat treatment temperature. Clear evidence for a non-leachable (strongly bound) chloride species on the PuO_2 surface is found from the thermal treatments. The lattice parameter decreases with increasing heat treatment temperature, reflecting annealing of structural defects caused by over 35 years of radiation damage, with no change in the fcc $Fm\bar{3}m$ crystal structure. Heating chloride-contaminated PuO_2 powder to ~230 °C and cooling back to ambient temperature in a sealed vessel reveals the production of H_2, He, NO and CO gases. Water adsorption/desorption behaviour with the untreated PuO_2 powder is remarkably different than PuO_2 which had previously been heat treated at 700 °C. From thermal treatments in open and sealed systems it is concluded that water and chloride co-adsorb and interact on the PuO_2 surface and each affects the adsorption/desorption behaviour of the other. These data also support practical considerations for repackaging of chloride-contaminated PuO_2 for long term safe and secure storage at Sellafield.

Keywords: *chloride, plutonium dioxide, water, adsorption, desorption, thermal treatment*

Highlights:

- First study of UK chloride-contaminated PuO_2 retrieved from storage
- >700 °C needed to volatilise chloride efficiently
- Evidence of leachable and non-leachable species on PuO_2 surface
- Unusual water adsorption behaviour on chloride-contaminated PuO_2

1. Introduction

Plutonium dioxide (PuO_2), produced from the reprocessing of spent nuclear fuel, has been safely and securely stored in the UK for over fifty years, awaiting either reuse in mixed oxide (MOX) fuel or disposal in a geological disposal facility (GDF) [1–6]. Processing and storage of this material takes place at the Sellafield nuclear fuel reprocessing and decommissioning site in Cumbria. The majority of the inventory is high purity PuO_2 from reprocessing but a small fraction of the inventory has become contaminated with chloride. These legacy materials, dating mainly from the early 1970s, were stored in nested metal containers with a polyvinyl chloride (PVC) intermediate layer between the inner and outer cans. The chloride contamination is due to thermal and radiolytic degradation of the PVC bags, forming $HCl_{(g)}$, which has been adsorbed onto the surface of the plutonium powder, together with water and other gases adsorbed from the air atmosphere by diffusion into these non-welded ('breathable') packages. This chloride and water-contaminated PuO_2 will require heat treatment in order to meet the conditions for acceptance (CFA) for repackaging and long term storage in modern facilities within welded cans. To underpin the design of the heat treatment process, it is necessary to characterise the chloride-contaminated powders and understand the process parameters which affect the partitioning of chloride between the product powder and off gas streams in a thermal treatment process. The properties of the product (heat treated) powder also need to be determined, in order to establish its suitability for long term storage and the ultimate disposition options. Based on previous simulant PuO_2 experiments, in which PuO_2 was artificially contaminated with chloride in the laboratory, increasing quantities of chloride were volatilised as the temperature of the heat treatment increased. Chloride adsorbed on the surface of the PuO_2 was determined by a caustic leaching method (this was termed 'leachable' chloride) and the experiments provided some evidence for a fraction of chloride that was strongly bound or 'non-leachable' when the powder was washed with NaOH solution [7].

CeO_2 is frequently used as a non-radiotoxic analogue to PuO_2, as it has the same fcc $Fm\overline{3}m$ crystal structure, +4 oxidation state and similar metal ion radius (Ce^{4+} = 0.97 Å and Pu^{4+} = 0.96 Å for 8 co-ordinate structures) [8–10]. Initial studies of HCl and water adsorbed on CeO_2 have been carried out [11] and these experiments proved that:

i. chloride is not incorporated into the CeO_2 crystal structure, as no crystalline phases other than the fcc $Fm\overline{3}m$ phase of CeO_2 are present,
ii. the sorption mechanisms of water and chloride are linked and
iii. heat treatment at 900 °C removes chloride from the surfaces of high and low specific surface area CeO_2 particles (58 and 2 $m^2\ g^{-1}$, respectively).

As indicated above, the CeO_2 studies were then extended to cover the interactions of chloride and water with PuO_2, using samples of high purity PuO_2 ('Magnox PuO_2') obtained from the reprocessing of spent Magnox fuel (a uranium metal fuel inside magnesium alloy cladding) which were artificially contaminated with chloride and humidified in the laboratory [7]. The aims were to establish the likely behaviour of chloride-contaminated PuO_2 in heat treatment, changes in properties before and after heat treatment, and to determine any similarities between the PuO_2 and CeO_2 analogues. This work showed that no crystal phase change is observed between chloride-contamination, humidification and heat treatment of the PuO_2 samples. Self-irradiation damage, caused by α-decay, is annealed at high heat treatment temperatures. The PuO_2 crystallites grow at temperatures higher than the original calcination temperature. A fraction of the chloride adsorbed onto the PuO_2 surface

is stable with respect to heat treatment, but is leachable with caustic solution at ambient temperature. We concluded that variations in PuO_2 specific surface area and production/storage history resulted in differences in behaviour, with respect to chloride desorption. These differences are likely to be accentuated when moving from studies of simulants produced in the laboratory to actual legacy chloride-contaminated materials retrieved from stores by, for instance, the differences in the chloride sources (dry HCl vapour versus *in situ* PVC degradation), radiation damage, storage temperature, the adsorption of atmospheric gases onto the surface and lengthened timescales of storage. Thus, the behaviour observed with simulants may not be fully representative of the stored high chloride materials. These experiments also suggested that the use of CeO_2 as a surrogate material for PuO_2 is of limited value in this case, as despite some similarities between the materials described above, substantial variations exist such as the differences in redox properties and self-irradiation effects [12].

This paper now reports the first studies on legacy chloride-contaminated PuO_2 powder retrieved from Sellafield stores, aiming to establish the likely inter-linked adsorption and desorption behaviours of chloride and water and their stabilities over a broad temperature range of relevance to the development of the heat treatment process. High temperature furnace experiments were carried out to study chloride-sorption, and lower temperature pressure vessel experiments were carried out to study water-sorption.

2. Experimental

Plutonium is an α-emitter, which presents both radioactivity and toxicity hazards. Manipulation and handling of these materials were performed only by qualified personnel in licensed radiological facilities.

2.1 Materials

A can of chloride-contaminated PuO_2 powder was retrieved from the Sellafield stores and opened. A series of sub-samples (~20g) were taken from the can and stored in small aluminium screw-top containers. These samples were transferred to the laboratories and held in nitrogen or argon inerted glove boxes before being moved to an air atmosphere glove box for the experimental programme. No other pre-processing was applied to these samples prior to the experimental programme. The material had been produced on an old finishing line by calcination of the plutonium (IV) oxalate precipitate at ~550 °C in 1980 and the plutonium isotopics are given in Table 1 following the original manufacture (measured) and at the start of the experimental programme (calculated). The specific surface area of the PuO_2 before heat treatment was determined by BET analysis using nitrogen as the adsorbate gas and measured to be 4.3 ± 0.9 $m^2\ g^{-1}$. The loss on heating (LOH) at 950 °C in argon was measured as 2.55 ±0.05 wt.%.

Table 1: Original plutonium isotopic analysis compared to calculated isotopics in 2016

Isotope	13/01/1981	30/6/16
U-234	0	0.05
U-235	0	0.07
U-236	0	0.09
Np-237	0	0.13
Pu-238	0.19	0.14
Pu-239	70.69	70.62
Pu-240	23.58	23.49
Pu-241	4.51	0.81
Pu-242	1.03	1.03
Am-241	0	3.57

2.2 Thermal treatments

Five samples (0.5 or 1 g aliquots of PuO_2) to be heat treated were poured into a borosilicate glass tube and inserted into a vertical tube furnace (1,000 °C INSTRON, UK) in an air atmosphere radiochemical (negative pressure) glove box. Based on preliminary experiments, the airflow was set to 250 mL min^{-1} to ensure adequate purging and capture of HCl and the furnace was heated to the specified temperature (400, 500, 600, 700, 800 or 950 °C) at 10 °C min^{-1}, then held at temperature for 2 hours. The furnace was then switched off and the powder was left to cool naturally to ambient temperature overnight, with the air flow maintained for the first hour of cooling. The effluent gas was passed through an NaOH trap (25 mL, 0.5 mol L^{-1}). Once the apparatus had cooled, the trap was emptied and washed out with ultra high quality water (2 x 10 mL). The thermal treatment experiments were essentially the same as those reported previously for the simulant studies [7].

2.3 Determination of chloride

A subsample of the NaOH solution from the trap solution (4 mL) was analysed for chloride by ion chromatography (IC) before and after heat treatment. Subsamples of PuO_2 powder were also taken before and after heat treatment, added to 4 mL of fresh NaOH solution, shaken, left for a few days to separate and the supernate filtered for IC, using an Anotope inorganic alumina membrane filter (pore size = 0.2 µm and diameter = 10 mm). IC was performed using a Dionex DX-500 with an AS18 column and a mobile phase of NaOH (0.023 mol L^{-1}) (current = 76 mA, flow rate = 1.30 mL min^{-1} and conductivity stabilised at <5 µS). Standards of 2, 5, 7 and 10 ppm Cl^- were used. The samples were diluted in ultra high purity water by a factor of 100 prior to analysis. Precision of the IC analysis was checked by triplicate analyses of selected samples (*e.g.* 3797, 3747, 3773 ppmCl) and also three replicate experiments at the same temperature using simulant samples gave good reproducibility (4000 ±78, 2σ) [7].

2.4 PuO_2 characterisation

Powder X-ray diffraction (XRD) analysis of the PuO_2 powders involved encapsulation of the oxide in epoxy resin. The methods have been described previously [7]. XRD patterns were recorded (Brücker D8) with step size = 0.02° and time per step = 9 s (2θ = 25-58°) and 18 s (2θ = 58-145°). Crystallite sizes, lattice parameters and uncertainties were obtained from the XRD patterns using Topas software [13].

2.5 PuO_2 – water interactions

The desorption/adsorption of surface species on the contaminated PuO_2 was investigated by heating a quantity of powder in a sealed vessel with and without small additions of water (typically 0.05 mL). The contaminated PuO_2, ~10 g, was placed inside a custom-design pressure vessel (LBBC Baskerville, Leeds) with a volume of 41.0 ± 1.2 cm^3. The sealed pressure vessel was heated inside a furnace (LBBC Baskerville, Leeds) with the whole experiment carried out in an argon atmosphere glove box. The target temperature of the furnace was maintained for 4 hours before heating was turned off, allowing the furnace to cool naturally to room temperature. The vessel temperature and pressure were recorded throughout the heating and cooling cycle.

In the first series of experiments untreated PuO_2 powder was heated to successively higher temperatures of 100, 150, 200 and 230 °C. The 230 °C cycle was carried out twice. After the final heating the head space gas in the vessel was sampled for analysis by gas chromatography (GC) using a Varian 490 micro GC with a 5Å molecular sieve column operating with an argon carrier gas, column temperature of ~90 °C and a thermal conductivity detector. Subsequently, 0.05 mL water was added to the vessel and the heating cycles were repeated with peak temperatures of 150 and 230 °C. Note that to maintain a safe operating envelope, ensuring strict compliance with the maximum permitted temperature in the 'Baskerville' vessel that is allowed under the safety case for its use in a plutonium glove box, the upper temperature was set between 220 and 240 °C for all experiments. This delivers a sufficient range of relative humidities within the vessel to study the physi-sorption of water on the PuO_2 surface.

In a second series of experiments, PuO_2 that had previously been heat treated at 700 °C in air in the tube furnace (following the procedure described in section 2.2) was heated in the sealed reactor to a temperature of 225 °C twice. After the second cycle, the vessel was opened and 0.05 mL water was added and the heating to 225 °C repeated.

3. Results

3.1 Thermal treatments

3.1.1 Ion Chromatography

The leachable chloride content on the untreated PuO_2 solid is ~5,400 ppm, as measured by caustic leaching and IC. This equates to an average of 2.9 monolayers (ML) of leachable chloride present on samples of untreated, chloride-contaminated PuO_2 before heat treatment (calculated using Eq. 1):

$$ML = \frac{mol_{adsorbed}}{n_m} \quad \textbf{(1)}$$

where $mol_{adsorbed}$ = number of moles of chloride adsorbed to the PuO_2 (determined from the chloride concentrations in the leached solutions) and n_m = number of moles of chloride per monolayer. The mass capacity for HCl on the PuO_2 surface is assumed to be 0.446 mg m^{-2}, compared to 0.22 mg m^{-2} for a water molecule [14]. That is, it is assumed that the surface area occupied by HCl on the PuO_2 surface is the same as for a water molecule. This is explained in more detail in ref. [7]. The uncertainty (± 9.3%) in the IC results shown are due to overall contributions from variations in the experiments as well as inherent heterogeneity in the powder, as chloride exposure varies through

the powder within the can due to diffusion of HCl from outside the can into the powder during storage, despite mixing after sub-sampling.

The amount of volatilised chloride present in the caustic trap after heating compared with before heating is calculated using Eq. 2, and is shown in Fig. 1.

$$Volatilised\ leachable\ chloride\ (\%) = \frac{(FC - SC)}{SS} x100\% \quad \textbf{(2)}$$

The mass of chloride in the caustic trap after heat treatment is the final caustic (FC) and the mass of chloride in the caustic trap before heat treatment is the starting caustic (SC). The mass of leachable chloride on PuO_2 before heat treatment is the starting solid (SS). The amount of chloride volatilised increases with heat treatment temperature. There is no discernible difference in the percentage of chloride volatilised from either the 0.5 or 1 g samples of PuO_2. In Fig. 1, 100% represents the chloride which is leachable on the untreated solid; that is, the measurement from the leached solid made before heat treatment. It is clear from the results that above 700 °C the volatilised chloride measured is more than 100% of the initial leachable chloride. This must infer that the total inventory of chloride in the solid is greater than that measured just by leaching with NaOH before heat treatment and that some of this 'non-leachable' chloride component is volatilised during the thermal treatments, at least above 700 °C.

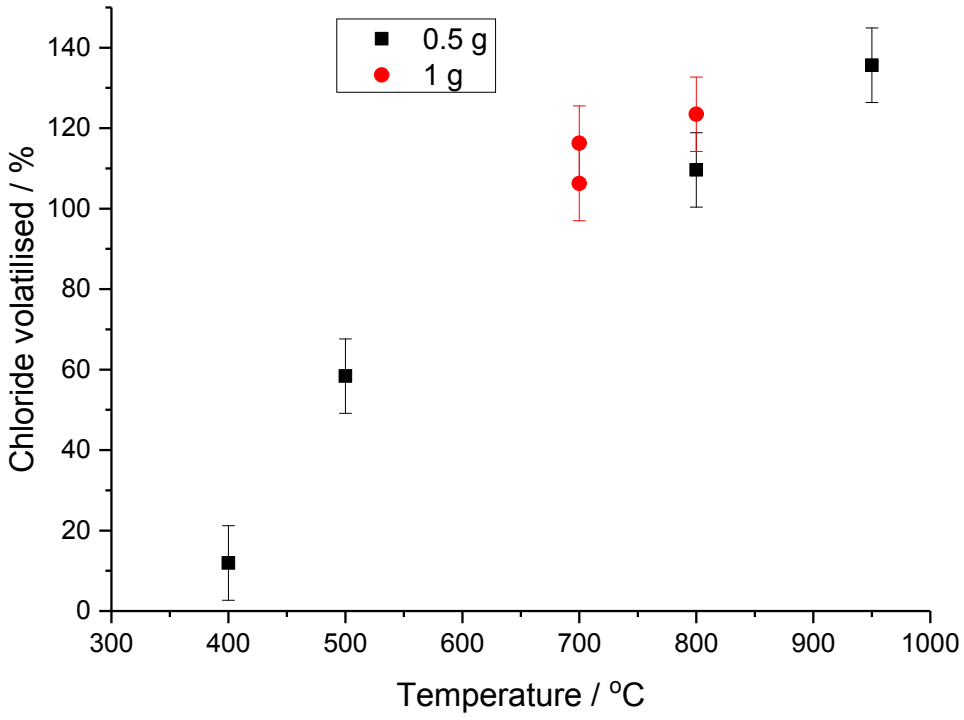

Figure 1: The percentage of chloride volatilised and trapped in the NaOH solution post-heat treatment, *c.f.* the leachable chloride on the solid PuO_2 pre-heat treatment.

Fig. 2 shows the volatilised and leachable chloride concentrations for the 0.5 g and 1 g samples measured after heat treatment relative to leachable chloride before heat treatment, which is taken

as 100%. It is seen that the leachable fraction on the solid decreases and the volatilised fraction increases with increasing heat treatment temperature. >100% of the initial leachable chloride was recovered at higher heat treatment temperatures in these samples compared to lower heat treatment temperatures where <100% recoveries were obtained. The percentage of leachable chloride remaining decreases with increasing temperature, reaching almost zero at 950 °C. These data infer that heating up to 700 °C causes conversion of some of the leachable chloride initially present on the sample to a non-leachable form. However, this non-leachable form of chloride may still be volatilised, and at 700 °C and above, volatilisation is the dominant process. Also, as noted above, some non-leachable chloride species must be present initially in the powder as >100% recoveries are obtained at higher temperatures.

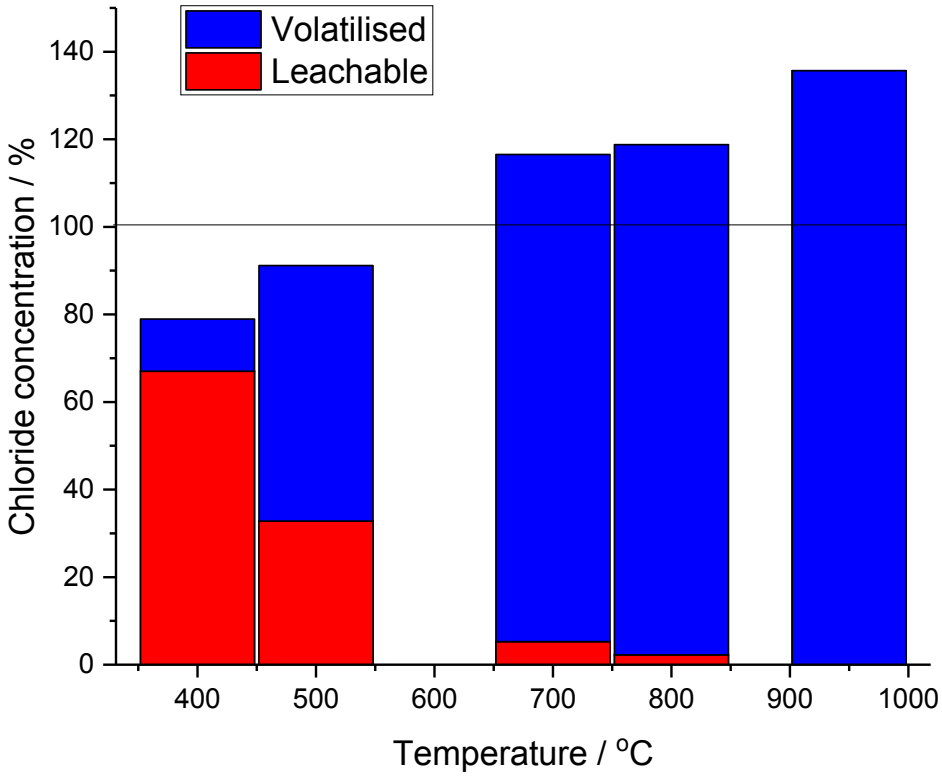

Figure 2: The average percentage of chloride present in leachable and volatilised fractions, following heat treatment at a range of temperatures from the 0.5 and 1 g PuO_2 starting material samples, where 100% is leachable chloride measured from untreated PuO_2 samples.

3.1.2 X-Ray Diffraction

Powder XRD patterns of chloride-contaminated PuO_2 before and after heat treatment at 400, 600, 800 and 950 °C are shown in Fig. 3; lines for a reference PuO_2 sample are also given [15]. No additional phases are present in either the untreated or heat treated samples. The crystallite sizes (calculated from the peak widths, using the Scherrer equation) increase with increasing heat treatment temperature, almost doubling in size following treatment at 950 °C (Fig. 4). The Bragg

peak positions shift for each heat treatment temperature as a consequence of the lattice parameters decreasing with increasing temperature.

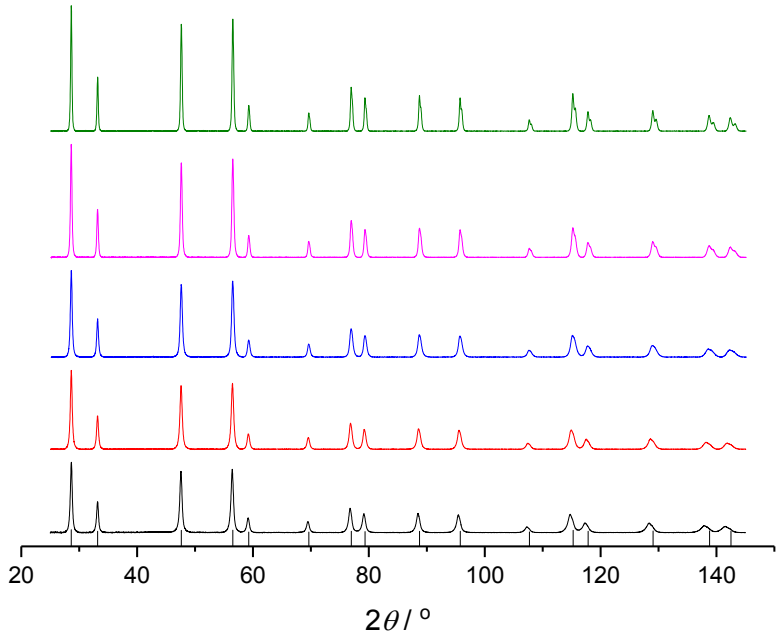

Figure 3: Powder XRD patterns of the contaminated Magnox PuO_2 untreated (black) and heat treated at 400 (red), 600 (blue), 800 (pink) and 950 °C (green). Reference lines for PuO_2 are also shown (R. Roof, Los Alamos).

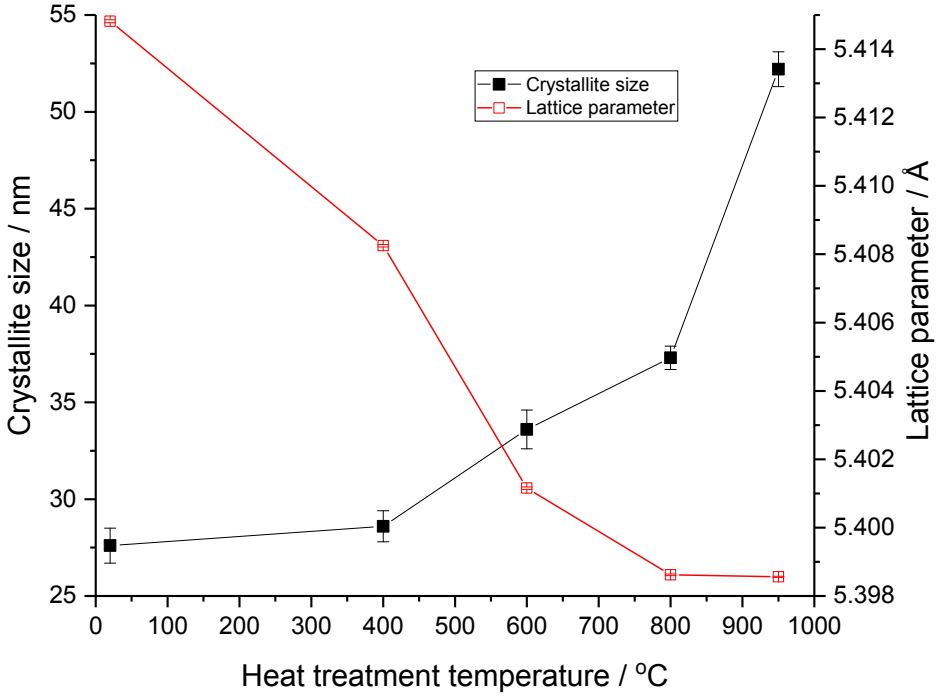

Figure 4: Crystallite sizes and lattice parameters obtained from the XRD patterns in Fig. 3.

3.2 PuO_2 – water interactions

3.2.1 Sequential heating of PuO_2 powder in the pressure/temperature 'Baskerville' vessel

An example of the recorded pressure variation with temperature for untreated, chloride-contaminated PuO_2 is shown (Fig. SI1). The heating/cooling curves show a hysteresis due to non-isothermal conditions in the heating cycle. In practice, heating measurements were used only for monitoring the progress of the experiment. In the analyses of data, the heating cycles are thus disregarded and so are not included in the remaining figures.

Firstly, with heating it had been surprisingly observed in a preliminary test that non-condensable gas was produced; hydrogen and helium were quantitatively measured in this experiment (Table 2). This was investigated further by running successive cycles with increasing peak temperatures up to 230 °C (Fig. SI1). The quantity of non-condensable gas increased as the furnace temperature was increased. The final pressure increases after each cycle compared to the starting pressure, even after heating the powder to 230 °C a second time; that is, there was no observed peak relating to a release at a specific intermediate temperature. The total pressure increased due to the non-condensable gas produced at ambient temperature over the five cycles is 0.056 MPa. The gas produced was qualitatively analysed by micro-gas chromatography (μGC) and found to contain He, H_2, N_2, NO and CO (Fig. SI2) although the sum of pressure calculated from the measured concentrations of these species cannot account for the majority of the gas produced. It must be assumed that gases which could not be separated and detected by μGC were also present. For example, CO_2 is likely to have adsorbed onto the surface during storage but would not be detected using the molecular sieve column if it desorbed.

Table 2: Hydrogen and helium analyses from a Baskerville experiment with untreated chloride-contaminated PuO_2 (* = average of two samples)

Hydrogen		Helium	
ppm	μmol / gPuO_2	ppm	μmol / gPuO_2
4500*	1.4*	520	0.16

Secondly, the monolayers of water (ML(H_2O)) adsorbed to the surface of the PuO_2, were calculated from the pressure measurements in Fig. SI1. The measured pressure is then used to calculate the moles of water vapour in the vessel; the difference between the total estimated moles of water in the vessel (adsorbed water and water added to the vessel in the later wet experiments) and the moles of water vapour then gives the moles of adsorbed water. Using Eq. 1 (with water as the adsorbent), the adsorbed moles can be converted to adsorbed monolayers of water. The mass capacity of water on PuO_2 is taken as 0.22 mg m^{-2} for a single monolayer [16]. Fig. 5 illustrates the variation of ML(H_2O) with the relative humidity (RH) in the vessel for the second cycle run to the maximum temperature (230 °C). RH is calculated from the ratio of the measured water vapour pressure and the saturated vapour pressure at the corresponding temperature.

This curve is compared with results obtained by Paffett *et al.* [14] who has previously reported the results of a similar study of water desorption from PuO_2 at Los Alamos National Laboratory and fitted data to the BET isotherm ([14,15] and references therein). The key point here is that the shapes of the curves are different. Much more water is adsorbed onto the chloride-contaminated

PuO_2 than the pure PuO_2 used by Paffet *et al*. (for RH <0.7). Whilst there maybe differences in the materials used (*e.g*. surface area, porosity, morphology and isotopics) it is unlikely that these differences account for the significantly greater affinity for water adsorption seen here with the chloride-contaminated PuO_2.

The literature describes clear distinctions between strongly adsorbed and weakly adsorbed water layers, although the exact nature of these layers is still a matter of debate – see section 4.2 [15]. Table 3 gives the estimated number of strongly adsorbed monolayers, estimated as the intercept of the curves at 0% RH determined using polynomial lines of best fit (see Fig. 5). The intercept is calculated as 2.7 ML(H_2O); the monolayers above this number are more weakly bound and represent the water layers that adsorb and desorb during the Baskerville experiment.

The maximum number of monolayers able to adsorb to the PuO_2 surface, based on the sum of the initial measured water content of the PuO_2 (by LOH at 950 °C, see section 2.1) and available moles of water added to the vessel, are given in Table 3, as are the number of strongly adsorbed monolayers estimated as the intercept of the curves at 0% RH, using polynomial lines of best fit (see Fig. 5). The literature describes clear distinctions between strongly adsorbed and weakly adsorbed water layers although the exact nature of these layers is still a matter of debate – see section 4.2 [15]. With the untreated chloride-contaminated samples this gives an estimate of 2-3 ML(H_2O) for the strongly bound fraction; the monolayers above this number are more weakly bound and represent the water layers that adsorb and desorb during the Baskerville experiment.

In the experiments with an aliquot of water added to the untreated chloride-contaminated PuO_2 powder sample, a smaller amount of non-condensable gas was produced (pressure increase inside the vessel = 0.021 MPa). This indicates that desorption of adsorbed gases (other than water) from the PuO_2 surface was still incomplete and possibly influenced by addition of water. The cumulative increases in pressure for successive dry and then wet cycles are illustrated in Fig. 6, noting that the wet cycles were performed on the same material following on from the dry cycles.

As before, the pressure/temperature measurements were used to calculate the monolayers of water adsorbed to the PuO_2 surface during the cooling cycles (Fig. 5, 230 °C run only). The key observations in this experiment are that the curves do not overlap; the slopes are comparable in the region of low RH, and at higher RH the approach towards condensation is seen in the experiment with water added. The slope of the plot for the chloride-contaminated PuO_2 is consistently higher than reported in the results of Paffett *et al*. [14] at RH <0.7.

As before, the monolayers of water which are strongly adsorbed to the PuO_2 can be calculated by a polynomial extrapolation back to 0% RH. The data for the full heating cycles are given in Table 3. This again highlights a change in behaviour when water is added to the system, with an apparent increase in the strongly bound fraction.

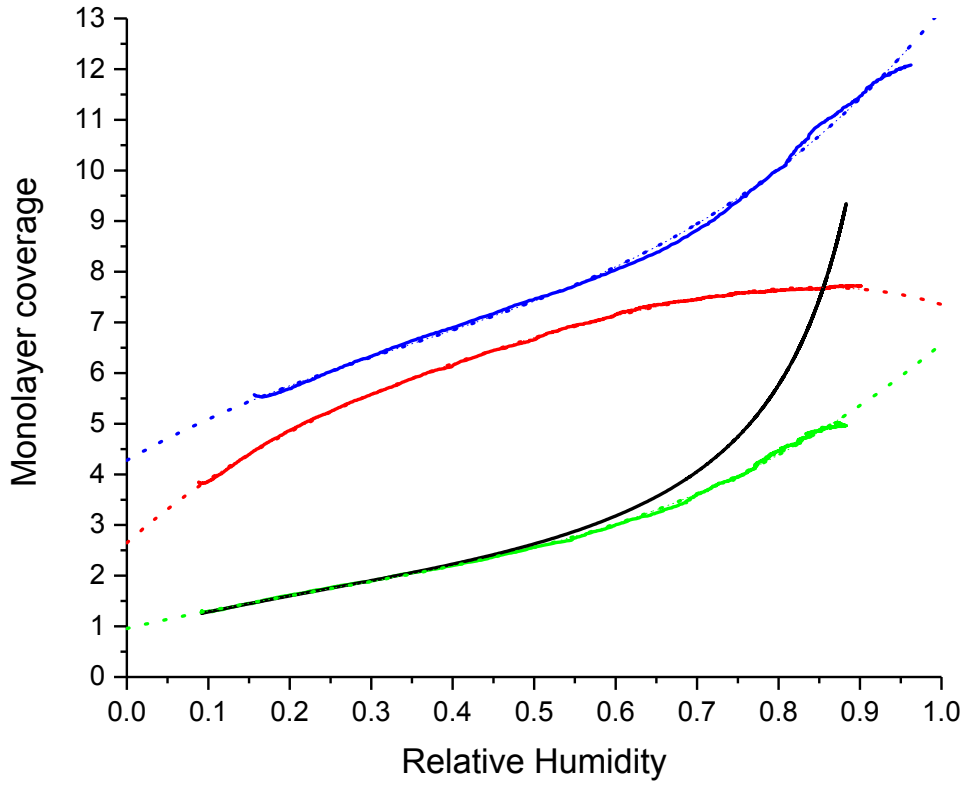

Figure 5: The calculated monolayer coverages of water on the untreated PuO_2 (red), untreated PuO_2 with 0.05 mL water (blue) and PuO_2 heat treated at 700 °C with 0.05 mL water (green), with data extrapolated to 0% RH (dotted lines), compared with the results obtained by Paffett *et al.* [14] (black).

Table 3: The monolayers of water strongly adsorbed at 0% RH calculated from extrapolation of experimental data obtained from full heating cycles, using a polynomial gradient (see Fig. 5) and maximum number of ML(H_2O) available for adsorption in the system.

Experiment	Max. ML(H_2O)	Max. Temp. / °C	ML(H_2O) at 0% RH
Untreated PuO_2 no added water (dry, 1st cycle)	8.2	226	2.4
Untreated PuO_2 no added water (dry, 2nd cycle)	8.2	225	2.6
Untreated PuO_2 added water (wet)	14.3	225	4.3
Heat treated PuO_2 added water (wet)	5.5	219	0.96

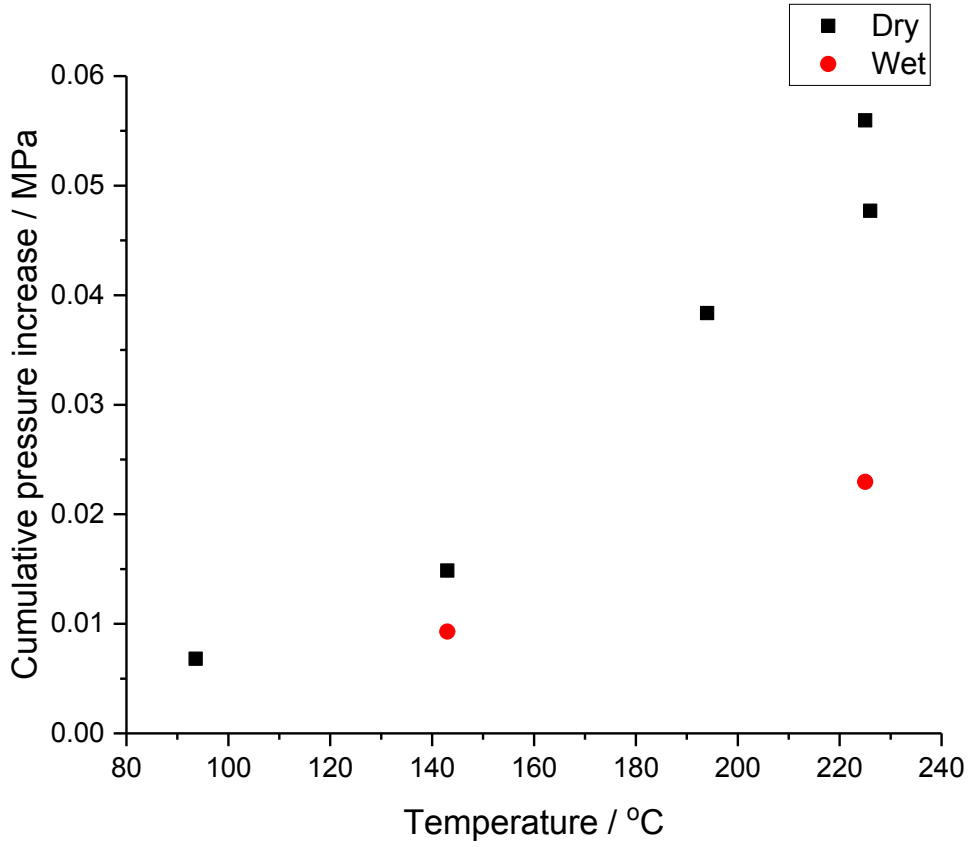

Figure 6: Cumulative pressure increase within the sealed vessel for the dry and wet experiments on untreated chloride-contaminated PuO_2 *vs.* maximum temperature of the cycle.

3.2.2 PuO_2 heat treated at 700 °C

Based on the above observation of the evolution of a non-condensable gas and in order to understand how water adsorption on the chloride-contaminated PuO_2 is affected by thermal treatment, a second study was initiated using a sample of PuO_2 which had previously been heat treated at 700 °C in air using the same methodology as described in section 2.2.

For the dry cycles it was apparent that (a) the pressure increase followed the ideal gas expansion as the material contains very little residual water following heat treatment at 700 °C and (b) a small amount of non-condensable gas was still released (0.009 MPa in the first heating cycle only). This may be due to either further release of helium from alpha decay or a small amount of gases (probably radiolysis products of air) that adsorbed onto the surface following heat treatment and before transfer into the inerted (argon atmosphere) glove box.

Repeating this experiment with the same PuO_2 in the presence of water produces a pressure rise, which is due to a non-ideal gas, condensable on cooling to ambient temperature in both cycles. Conversion of the experimental P/T data to the ML(H_2O) vs. RH in Fig. 5 shows a striking change in behaviour compared with the original untreated chloride-contaminated PuO_2 that was retrieved from stores. The water sorption behaviour now appears close to the results of Paffett *et al*. [14], at least below ~0.6 RH – there is some deviation at high RH but in this region the uncertainties in the method increase significantly and the influences of morphology, porosity *etc*. might increase.

3.2.3 Chloride analysis

Table 4 shows that the monolayers of chloride adsorbed to the untreated PuO_2 do not change significantly following dry and wet thermal cycling up to 225 °C. Given the data of Fig. 1 it is expected that chloride desorption at the temperatures reached in the Baskerville vessel will be very low; some changes in surface speciation with humidity, however, might be expected [7]. The chloride data obtained on the heat treated sample showed the expected reduction in leachable chloride due to the desorption that occurred during the heat treatment. There was a possible decrease following the experimental heating cycles with the untreated dry powder. This may reflect an inter-conversion between leachable and non-leachable species as, at these low temperatures, volatilisation is not expected. However, even if this has occurred, following the cycles with added water, the surface is obviously re-hydrated and the leachable chloride species returns to the value found before any Baskerville runs (0.6-0.7 ML(HCl)).

Table 4: Leachable chloride monolayers on the untreated and heat treated PuO_2 solids, measured before and after the dry and wet heating cycles.

PuO_2	Point of analysis	Chloride monolayers /ML
Untreated	Before dry cycles	3.1
Untreated	After dry cycles (before wet cycles)	3.2
Untreated	After wet cycles	3.3
Heat treated (700 °C)	Before dry cycles	0.64
Heat treated (700 °C)	After dry cycles (before wet cycles)	0.43
Heat treated (700 °C)	After wet cycles	0.70

4. Discussion

4.1 Surface chemistry

The results show that when the PuO_2 powder is heat treated at <700 °C, less than 100% of the chloride leachable before heat treatment is recovered from the leachable and volatilised chloride after heat treatment. Even though some chloride is volatilised at these lower heat treatment temperatures, a significant proportion of leachable chloride remains bound to the PuO_2. However, more than 100% of the initial (leachable) chloride is detected in the caustic trap post-heat treatment at higher temperatures, with margins exceeding possible errors (*c.f.* pre-heat treatment, Fig. 1). This suggests that there is a non-leachable chloride component either strongly bound on the surface or contained within the bulk PuO_2. It appears that heat treatment temperatures >700 °C can volatilise the non-leachable chloride species. This is influenced by weakening the interactions between the adsorbed chloride and the surface, the additional energy input to overcome the barrier and loss of surface sites as SSA decreases. For example, in Fig. 2, IC of the leachable chloride remaining on the surface after heat treatment at 950 °C reduces to almost zero, yet the percentage of chloride recovered from the caustic trap for this heat treatment temperature is 135% (*c.f.* the starting solid PuO_2). So, from the heat treatment data, there is a clear indication that there are chloride species adsorbed on the PuO_2 surface that are not leachable in dilute NaOH as well as leachable species. At lower furnace temperatures, in an open system, it seems probable that leachable species are

converted to non-leachable species. It is also possible that the humid atmosphere in the sealed system can re-hydrate the surface to regenerate leachable chloride species. The nature of these species requires the application of surface sensitive techniques such as infrared (IR) and Raman spectroscopies or X-ray photo-electron spectroscopy (XPS) and was not the object of this study. However, based on similar studies of chloride adsorption in the literature, dissociative adsorption of HCl, formation of a hydroxylated $Pu^{IV}(H_2O)^{+}Cl^{-}$ species and incorporation into the structure have been proposed as a hypothetical framework [7,18–25]. Other possibilities include an amorphisation of the surface to form PuO_{2+x} and radiation damage leading to defect formation. These sites could then be amenable to formation of PuO_xCl_y species. Since radiolytic degradation of plasticised PVC produces $HCl_{(g)}$ as the only chloride-containing contaminant, the presence of at least two forms of chloride on the PuO_2 surface highlights the complex chemistry of the PuO_2 surface [26–28]. It is not impossible that there are adsorbed organic chlorides from exposure to air atmosphere under the conditions of storage [23–25] although we see no evidence for this possibility as yet.

Previous work on chloride-contaminated CeO_2 analogues revealed that the chloride homogeneously covered all available surface area, including within pores, but this was volatilised to the extent that the chloride remaining on the particles was below the limit of detection using energy dispersive X-ray analysis after heat treatment at 900 °C, showing that heat treatment removes chloride from all metal oxide surfaces, both exposed on the exterior of aggregates and within the aggregates [11]. The amounts of leachable chloride in the samples presented here are similar to those of simulant PuO_2, which was contaminated with dry HCl gas and humidified in the laboratory, before being heat treated at various temperatures [7]. However, the profiles for the simulant heat treated samples are significantly different. This is undoubtedly due to the age (>35 years storage) and storage history of the samples (self-heating, breathable containers), resulting in different amounts of radiation damage to the lattice, changing particle morphology and the evolution over time of the adsorbed gases on the surface. These are conditions that cannot be replicated in a laboratory and, overall, it appears that neither of our previous studies generated wholly realistic simulants for the actual legacy chloride-contaminated PuO_2.

The thermal treatments in the open system and the mechanism of Parfitt *et al*. imply a role for water in the surface chemistry of chloride-contaminated PuO_2. The adsorption of water on pure PuO_2 is a field of long-standing debate. Stakebake defines three types of water adsorption to the PuO_2 surface: (i) chemisorbed water, which forms strongly bound hydroxyls by dissociative adsorption onto Pu and O, (ii) quasi-chemisorbed molecular water, which either singly or doubly hydrogen bonds to the hydroxyls and (iii) physisorbed molecular water, which hydrogen bonds to adsorbed molecular water [29]. Haschke and Ricketts suggest that one monolayer of water tenaciously chemisorbs to the PuO_2 surface at low relative humidity and another monolayer physisorbs by RH of 0.50 [15]. Stakebake and Veirs *et al*. suggest that the chemisorbed hydroxyls cannot be desorbed below 1,000 °C and Farr *et al*. report the ubiquitous presence of surface hydroxyls when PuO_2 is exposed to water vapour, through both molecular and dissociative adsorption, which remain on the surface up to 590 °C [30-31]. Wellington *et al*. suggest that the first adsorbed water monolayer is either dissociatively or molecularly bound, depending on the Miller index of the surface [32]. Theoretical studies by Tegner *et al*. report the highest temperature of desorption of the hydroxylated PuO_2 (1 0 0) surface to be 377 °C under a pressure of 5 bar, higher than the maximum temperature the powder was heated to in our P/T experiments of ~230 °C [33].

The co-adsorption of ~3 monolayers of chloride and other radiolysed gases adsorbed from the air on the untreated PuO_2, which has not been annealed, are the two main factors contributing to the differences between water sorption profiles in this experiment and previous theoretical and experimental data, such as the profile of Paffett *et al*. These differences lead to variations in the amount of adsorption sites available on the PuO_2 surface, such as increased oxygen vacancies within the crystal structure [34-35]. The P/T sealed vessel experiments show a significant evolution from a profile that is very different to the expected Paffett-type behaviour (untreated chloride-contaminated PuO_2, dry cycle) to profiles that are close to the expected behaviour after chloride-contaminated PuO_2 has been heat treated at 700 °C.

There is a clear implication that the presence of chloride (and possibly other adsorbates) on the surface changes the adsorption of water. The Baskerville experiments are consistent with literature that proposes multi-layer adsorption of water on PuO_2 [15].

We propose that the high chloride content present on the untreated PuO_2 surface (~3 ML) is closely associated with adsorbed water and, furthermore, can adsorb additional water under humid conditions leading to multiple layers of water adsorption in these powders. This is not observed in the 700 °C heat treated PuO_2 sample as much of the adsorbed chloride has been volatilised during heat treatment leaving only ~0.7 ML chloride on the surface. In this case, the water adsorption tends to behaviours expected for pure PuO_2 [14].

A final question relates to the nature of the strongly bound water layer. The P/T method with the Baskerville vessel used here was not designed to probe this layer but extrapolation of the experimental curves to 0 RH lead to estimates for the thickness of the strongly bound water layers. Paffett *et al*. have reported that they saw a slow change in their P/T cycles attributed to formation of a thickening hydroxide layer [14]. Other authors have also reported evidence for a transition from weakly bound to strongly bound water over time. The strongly bound layers calculated in these experiments are higher than expected from normal chemi-sorption models and appear to change depending on the conditions. However, unlike literature data, they are probably attributable to the formation of mixed chloride/water species that are more difficult to remove than simple physi-sorbed water layers, *i.e.* there is some chemical interaction between water and chloride when adsorbed on PuO_2. Finally, other adsorbed gases are present on the chloride-contaminated PuO_2, including NO_x from the radiolysis of nitrogen. These species will also most likely interact with chloride and water, complicating the surface chemistry. One conclusion is that the surface will be highly acidic.

4.2 Gas evolution

Non-condensable gas was evolved from the untreated sample when heated in the Baskerville vessel at varying temperatures. A small amount of helium was present in the gas sample; this is due to α-decay of the plutonium isotopes during decades of storage and hold up of part of the helium formed in the PuO_2 matrix. It is interesting that heating even at these relatively low temperatures can cause helium diffusion out of the matrix. The production of H_2 measured by GC is attributed to the radiolysis of adsorbed water on the PuO_2 surface as it is in agreement with theoretical studies [30,31] and experimental studies by Veirs *et al*. [34] Sims *et al*. [37] and references therein. Some fraction of the NO and CO species adsorbed to the PuO_2 surface were volatilised in this experiment, but are not oxidised, as these experiments were carried out in an argon atmosphere glove box. NO_x

is known to be formed from radiolysis of N_2 in the gas phase [38-40]. The maximum pressure reached at 230 °C was 0.505 MPa and more gas (particularly helium from within the pores) would have evolved, had the 230 °C cycle been repeated more times or the peak temperature been higher.

With thermal treatment at 700 °C under an air atmosphere, adsorbed volatile species, such as H_2O, CO_2 and NO_2, will have mostly been desorbed together with a substantial part of the chloride inventory [7]. However, after the PuO_2 sample was heat treated at 700 °C, it was stored in an air atmosphere glove box, potentially allowing oxidised gaseous species, such as H_2O, N_2 and CO_2, to re-adsorb to the PuO_2 surface (N_2 is subject to radiolysis and adsorption as NO_x) [7]. The non-condensable gas released during the first Baskerville run on the heat treated sample can likely be attributed to desorption of the species adsorbed during this short period of interim storage as no more gas is evolved on heating the powder a second time. This supports the assumption that thermal treatment followed by storage under dry argon is needed to stabilise the chloride-contaminated PuO_2.

None of the species detected by gas chromatography are of sufficient concentration to explain the total pressurisation observed in runs with untreated chloride-contaminated PuO_2. Therefore, dominant species produced by heating the PuO_2 must be a species such as CO_2, N_2O or Cl_2, which cannot be separated on the molecular sieve column.

4.3 X-Ray Diffraction

The XRD pattern of the chloride-contaminated PuO_2 (Fig. 3) shows only the fcc $Fm\overline{3}m$ crystal phase and no phase change as the sample is heated. The crystal sizes of the untreated PuO_2 are 27.6 (± 0.9) nm (Fig. 4). This is similar to previous work carried out on simulant PuO_2, which was contaminated with dry HCl vapour and humidified and yielded a crystal size of 29.1 (± 0.8) nm. The PuO_2 crystallite size increases as the heat treatment temperature increases, especially above 600 °C, since the powders were originally calcined at 550 °C. The maximum crystal size for PuO_2 powders heat treated at 950 °C is 52.2 (± 0.9) nm.

The lattice parameters, calculated from the XRD patterns (Fig. 4), show that the lattice contracts as the heat treatment temperature increases. The lattice parameter for the 950 °C heat-treated PuO_2 powder sample (5.3986 Å) is larger than that reported by Farr *et al.* (5.3975 Å) for stoichiometric PuO_2 and by Chikalla *et al.* (5.3954 Å) for $^{238}PuO_2$; however, the sample heat treatment (950 °C) was at a lower temperature than that used to anneal $^{238}PuO_2$ (>1,000 °C) [30,41]. The lattice has expanded over time, due to radiation damage from alpha decay of the Pu isotopes; heat treatment of the powders at higher temperatures anneals these lattice defects and causes the lattice to contract [41-43]. The lattice parameter of the untreated, chloride-contaminated PuO_2 (5.4148 Å) is larger than that of simulant PuO_2, which had been contaminated with dry HCl vapour and humidified under laboratory conditions (5.4062 Å), as the PuO_2 simulant material was of recent production and the lattice parameter had not reached the steady state from radiation damage [7].

5. Conclusions

The effects of heat treatment on chloride and water-contaminated PuO_2 have been presented. As expected, high heat treatment temperatures of 700, 800 and 950 °C volatilise almost all of the leachable chloride present on the 0.5 g and 1 g PuO_2 starting material sample surfaces before heat

treatment. More interesting is that chloride recoveries change from <100%, relative to initial leachable chloride, at lower heat treatment temperatures to >100% at high temperatures providing clear evidence for a 'non-leachable' fraction and probable inter-conversion between leachable and non-leachable fractions depending on the surface hydration. This is supported by lower temperature heating cycles in a sealed system (humid atmosphere). Further studies using spectroscopic techniques such as IR and XPS are needed to investigate the surface speciation and chemical interactions between water and chloride. XRD of the PuO_2 powders shows that heat treatment leads to an increase in crystallite size and a smaller lattice parameter due to annealing radiation damage but there is no evidence for bulk phases other than PuO_2. Untreated and heat treated chloride-contaminated PuO_2 powders behaved remarkably differently in thermal cycling experiments in a sealed vessel with regards to water adsorption and provided evidence that it is the presence of chloride on the untreated sample that contributes to these differences. Estimates of the number of layers of strongly bound water have also been made and are ~3 ML(H_2O) which compares with ~3 ML chloride present initially for the untreated sample. Overall, the data here present strong evidence that water and chloride co-adsorb on PuO_2 and that the sorption/desorption behaviours of each are affected by the other. These data also support practical considerations for repackaging of chloride-contaminated PuO_2 for long term safe and secure storage at Sellafield.

Acknowledgements

We thank the EPSRC and Sellafield Ltd. for a studentship (to SSH). All experiments were carried out with the aid of Kevin Webb, Colin Gregson, Stacey Reilly, Catherine Campbell, Hannah Colledge, Josh Holt and Bliss McLuckie at the National Nuclear Laboratory Central Laboratory, Sellafield, Cumbria, UK; access (for SSH) was funded by the Nuclear Decommissioning Authority. We also thank John Waters (University of Manchester) for his guidance with powder X-ray diffraction.

Data availability

The raw/processed data required to reproduce these findings cannot be shared at this time as the data also forms part of an ongoing study.

References

[1] L. Cadman, A. Goater, Managing the UK Plutonium Stockpile, 2016. researchbriefings.files.parliament.uk/documents/POST-PN-0531/POST-PN-0531.pdf.

[2] Nuclear Decommissioning Authority, Progress on approaches to the management of separated plutonium, 2014. doi:21100718.

[3] Department of Energy and Climate Change, Management of the UK's plutonium stocks: A consultation on the long-term management of UK owned separated civil plutonium, 2011.

[4] N.C. Hyatt, Plutonium management policy in the United Kingdom: The need for a dual track strategy, Energy Policy. 101 (2017) 303–309. doi:10.1016/j.enpol.2016.08.033.

[5] P. Cook, H. Sims, D. Woodhead, Safe and Secure Storage of Plutonium Dioxide in the United Kingdom, Actinide Research Quarterly. August (2013) 20–25.

[6] R. Taylor, J. Hobbs, R. Orr, H. Steele, Characterisation of plutonium dioxide, Nuclear Future.

14 (2018) 40–50.

[7] S. Sutherland-Harper, C. Pearce, C. Campbell, M. Carrott, H. Colledge, C. Gregson, J. Hobbs, F. Livens, N. Kaltsoyannis, R. Orr, M. Sarsfield, H. Sims, H. Steele, I. Vatter, L. Walton, K. Webb, R. Taylor, Characterisation and heat treatment of chloride contaminated and humidified PuO2 samples, Journal of Nuclear Materials. 509 (2018) 654–666. doi:10.1016/j.jnucmat.2018.07.031.

[8] H.S. Kim, C.Y. Joung, B.H. Lee, J.Y. Oh, Y.H. Koo, P. Heimgartner, Applicability of CeO2 as a surrogate for PuO2 in a MOX fuel development, Journal of Nuclear Materials. 378 (2008) 98–104. doi:10.1016/j.jnucmat.2008.05.003.

[9] R.D. Shannon, Revised Effective Ionic Radii and Systematic Studies of Interatomic Distances in Halides and Chalcogenides, Acta Crystallographica Section A. 32 (1976) 751–767.

[10] M.C. Stennett, C.L. Corkhill, L.A. Marshall, N.C. Hyatt, Preparation, characterisation and dissolution of a CeO2 analogue for UO2 nuclear fuel, Journal of Nuclear Materials. 432 (2013) 182–188. doi:10.1016/j.jnucmat.2012.07.038.

[11] S. Sutherland-Harper, R. Taylor, J. Hobbs, S. Pimblott, R. Pattrick, M. Sarsfield, M. Denecke, F. Livens, N. Kaltsoyannis, B. Arey, L. Kovarik, M. Engelhard, J. Waters, C. Pearce, Surface speciation and interactions between adsorbed chloride and water on cerium dioxide, Journal of Solid State Chemistry. 262 (2018) 16–25. doi:10.1016/j.jssc.2018.02.018.

[12] J.C. Marra, Cerium as a surrogate in the Plutonium immobilization waste form, 2002.

[13] C.L. Corkhill, D.J. Bailey, F.Y. Tocino, M.C. Stennett, J.A. Miller, J.L. Provis, K.P. Travis, N.C. Hyatt, Role of Microstructure and Surface Defects on the Dissolution Kinetics of CeO2, a UO2 Fuel Analogue, ACS Applied Materials and Interfaces. 8 (2016) 10562–10571. doi:10.1021/acsami.5b11323.

[14] M.T. Paffett, D. Kelly, S.A. Joyce, J. Morris, K. Veirs, A critical examination of the thermodynamics of water adsorption on actinide oxide surfaces, Journal of Nuclear Materials. 322 (2003) 45–56. doi:10.1016/S0022-3115(03)00315-5.

[15] J.M. Haschke, T.E. Ricketts, Adsorption of water on plutonium dioxide, Journal of Alloys and Compounds. 252 (1997) 148–156. doi:10.1016/S0925-8388(96)02627-8.

[16] G.D. Parfitt, J. Ramsbotham, C.H. Rochester, Infra-red study of hydrogen chloride adsorption on rutile surfaces, Transactions of the Faraday Society. 67 (1971) 3100–3109. doi:10.1039/tf9716703100.

[17] P. Jackson, G.D. Parfitt, Infra-red study of the surface properties of rutile. Water and surface hydroxyl species, Transactions of the Faraday Society. 67 (1971) 2469. doi:10.1039/tf9716702469.

[18] J.W. Elam, C.E. Nelson, M.A. Tolbert, S.M. George, Adsorption and desorption of HCl on a single-crystal α-Al2O3(0001) surface, Surface Science. 450 (2000) 64–77. doi:10.1016/S0039-6028(99)01247-9.

[19] R. V Siriwardane, J.. Wightman, Interaction of hydrogen chloride and water with oxide surfaces, Journal of Colloid and Interface Science. 94 (1983) 502–513. doi:10.1016/0021-9797(83)90290-4.

[20] R.R. Bailey, J.P. Wightman, Interaction of gaseous hydrogen chloride and water with oxide

surfaces, Journal of Colloid and Interface Science. 70 (1979) 112–123. doi:10.1016/0021-9797(79)90014-6.

[21] M. Heuberger, G. Dietler, L. Schlapbach, New aspects in Volmer-Weber 3D growth: an XPS intensity study applied to thin films of Au and Ce on polypropylene, Surface Science. 314 (1994) 13–22. doi:10.1016/0039-6028(94)90209-7.

[22] B.M. Weckhuysen, G. Mestl, M.P. Rosynek, T.R. Krawietz, J.F. Haw, J.H. Lunsford, Destructive Adsorption of Carbon Tetrachloride on Alkaline Earth Metal Oxides, The Journal of Physical Chemistry B. 102 (1998) 3773–3778. doi:10.1021/jp980185k.

[23] K.H. Park, S.J. Oh, Electron-spectroscopy study of rare-earth trihalides, Physical Review B. 48 (1993) 14833–14842. doi:10.1103/PhysRevB.48.14833.

[24] J. Colombani, V. Labed, C. Joussot-Dubien, A. Périchaud, J. Raffi, J. Kister, C. Rossi, High doses gamma radiolysis of PVC: Mechanisms of degradation, Nuclear Instruments and Methods in Physics Research, Section B: Beam Interactions with Materials and Atoms. 265 (2007) 238–244. doi:10.1016/j.nimb.2007.08.053.

[25] I. Boughattas, E. Pellizzi, M. Ferry, V. Dauvois, C. Lamouroux, A. Dannoux-Papin, E. Leoni, E. Balanzat, S. Esnouf, Thermal degradation of γ-irradiated PVC: II-Isothermal experiments, Polymer Degradation and Stability. 126 (2016) 209–218. doi:10.1016/j.polymdegradstab.2015.05.010.

[26] A.H. Zahran, E.A. Hegazy, F.M. Ezz Eldin, Radiation effects on poly (vinyl chloride)-I. gas evolution and physical properties of rigid PVC films, Radiation Physics and Chemistry. 26 (1985) 25–32. doi:10.1016/0146-5724(85)90028-7.

[27] J.L. Stakebake, A Thermal Desorption Study of the Surface Interactions between Water and Plutonium Dioxide, The Journal of Physical Chemistry. 77 (1973) 581–586. doi:10.1021/j100624a003.

[28] D.K. Veirs, M.A. Stroud, J.M. Berg, J.E. Narlesky, L.A. Worl, M.A. Martinez, A. Carillo, MIS High-purity plutonium oxide metal oxidation product TS707001 (SSR123): Final report, 2017.

[29] J.D. Farr, R.K. Schulze, M.P. Neu, Surface chemistry of Pu oxides, Journal of Nuclear Materials. 328 (2004) 124–136. doi:10.1016/j.jnucmat.2004.04.001.

[30] J.P.W. Wellington, A. Kerridge, J. Austin, N. Kaltsoyannis, Electronic structure of bulk AnO2(An = U, Np, Pu) and water adsorption on the (111) and (110) surfaces of UO2 and PuO2 from hybrid density functional theory within the periodic electrostatic embedded cluster method, Journal of Nuclear Materials. 482 (2016) 124–134. doi:10.1016/j.jnucmat.2016.10.005.

[31] B.E. Tegner, M. Molinari, A. Kerridge, S.C. Parker, N. Kaltsoyannis, Water adsorption on AnO2{111}, {110}, and {100} surfaces (An = U and Pu): A density functional theory + U study, Journal of Physical Chemistry C. 121 (2017) 1675–1682. doi:10.1021/acs.jpcc.6b10986.

[32] D.R. Mullins, The surface chemistry of cerium oxide, Surface Science Reports. 70 (2015) 42–85. doi:10.1016/j.surfrep.2014.12.001.

[33] M.A. Henderson, C.L. Perkins, M.H. Engelhard, S. Thevuthasan, C.H.F. Peden, Redox properties of water on the oxidized and reduced surfaces of CeO2(1 1 1), Surface Science. 526 (2003) 1–18. doi:10.1016/S0039-6028(02)02657-2.

[34] D.K. Veirs, J.M. Berg, D.D. Hill, D.M. Harradine, J.E. Narlesky, E.L. Romero, L. Trujillo, K.V.J.

Wilson, Water radiolysis on plutonium dioxide: Initial results identifying a threshold relative humidity for oxygen gas generation, 2012.

[35] T.D. Chikalla, R.P. Turcotte, Self-radiation damage ingrowth in 238 PuO 2, Radiation Effects. 19 (1973) 93–98. doi:10.1080/00337577308232225.

[36] N.P. Turcottes, T.D. Chikalla, Annealing of self-radiation damage in 238 PuO2, Radiation Effects. 19 (1973) 99–108. doi:10.1080/00337577308232226.

[37] W.J. Weber, Alpha-irradiation damage in CeO2 , UO2 and PuO2, Radiation Effects. 83 (1984) 145–156. doi:10.1080/00337578408215798.

Supplementary Information

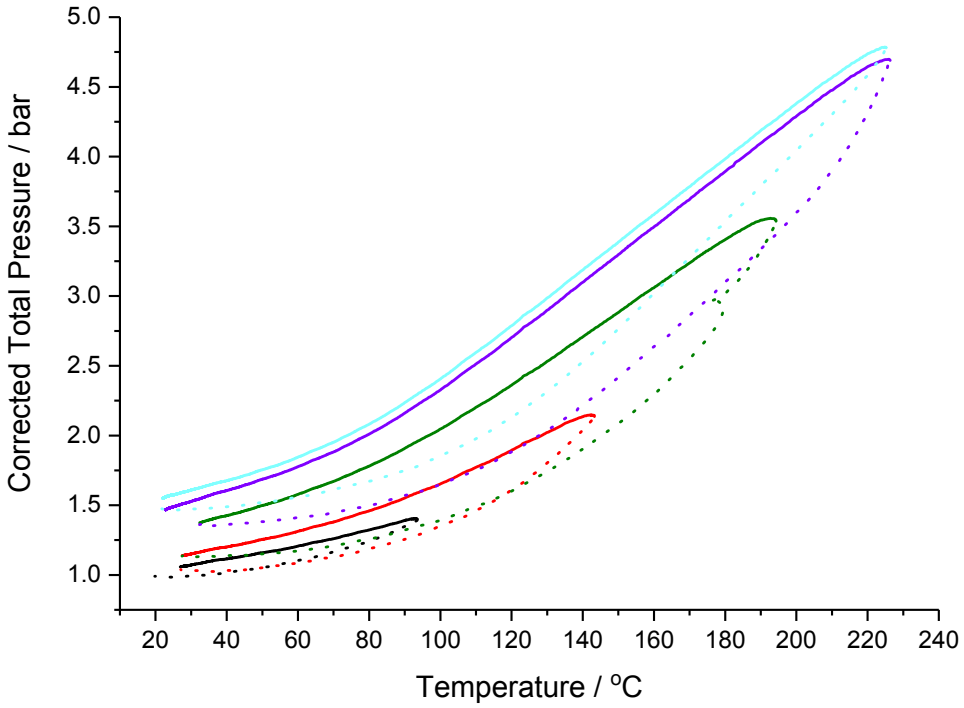

Figure SI1: Variation of pressure with temperature for contaminated Magnox PuO_2 inside the Baskerville vessel with maximum furnace temperatures of 100 (black), 150 (red), 200 (green) and 230 °C (two cycles, dark and light blue) without water (dotted line = heating curve and solid line = cooling curve).

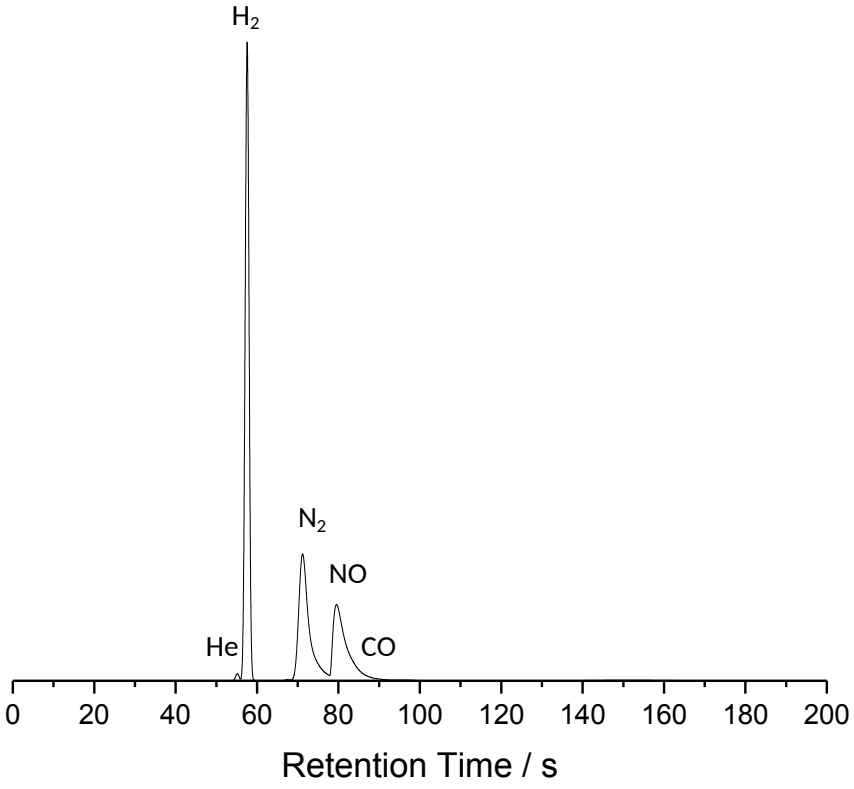

Figure SI2: Chromatogram of the gas sampled from the Baskerville vessel after heating/cooling cycles of dry chloride-contaminated PuO_2 (experiments illustrated in Fig. SI1). The N_2 detected is either due to contamination of the gas chromatography sample from air leaking into the glove box or contamination of the PuO_2 powder.

Highlights

- First study of UK chloride-contaminated PuO_2 retrieved from storage.
- >700 °C needed to volatilise chloride efficiently.
- Evidence of leachable and non-leachable species on PuO_2 surface.
- Unusual water adsorption behaviour on chloride-contaminated PuO_2.

Graphical Abstract

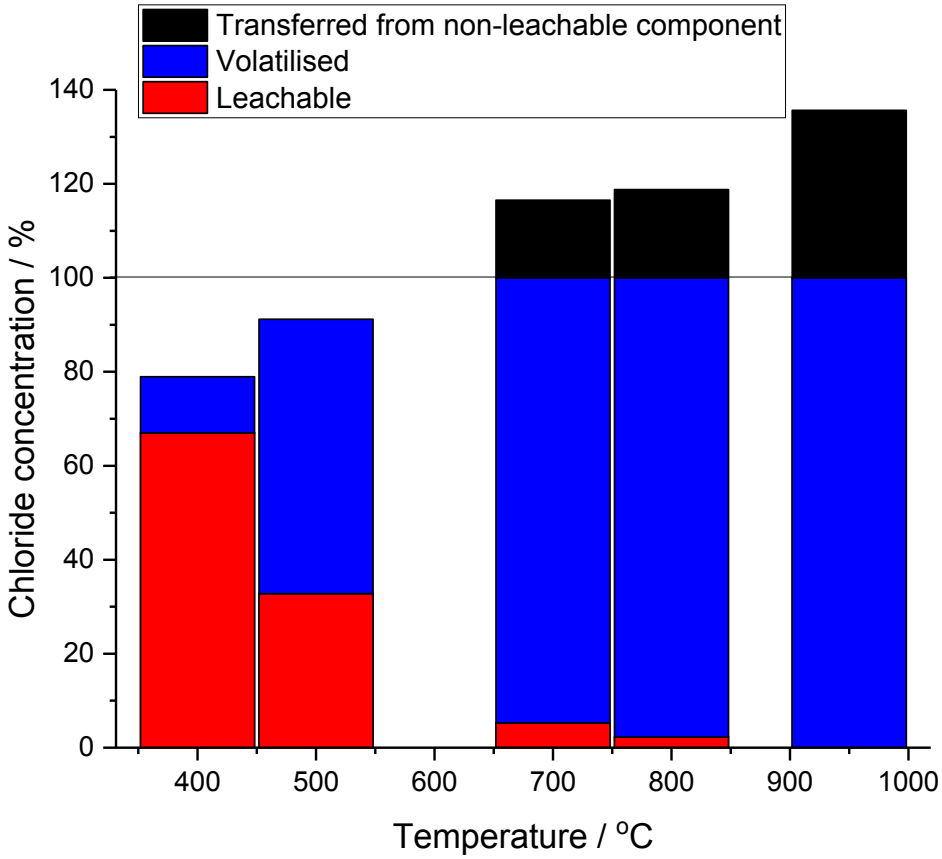

Interactions of HCl and H_2O with the surface of PuO_2

Sophie Sutherland-Harper[1], Francis Livens[1], Carolyn Pearce[1,2], Jeff Hobbs[3], Robin Orr[4], Robin Taylor[4], Kevin Webb[4] and Nikolas Kaltsoyannis[1]

[1]School of Chemistry, University of Manchester, Oxford Road, Manchester, M13 9PL, UK; [2]Pacific Northwest National Laboratory, Richland, WA 99354, USA; [3]Sellafield Ltd., Sellafield, Seascale, Cumbria, CA20 1PG, UK; [4]National Nuclear Laboratory, Central Laboratory, Sellafield, Seascale, Cumbria, CA20 1PG, UK

Abstract

In order to explore the potential of heat treatment to decontaminate Cl^-- and water-contaminated legacy plutonium dioxide (PuO_2) powders from the UK stockpile, samples have been heated in air from 400 to 950 °C. The amount of leachable chloride remaining on the PuO_2 particles after heat treatment decreases, and the amount of volatilised chloride (as measured by trapping in NaOH solution) increases, with increasing heat treatment temperature. High heat treatment temperatures are also capable of volatilising non-leachable chloride species from the PuO_2 solid. The lattice parameter decreases with increasing heat treatment temperature, reflecting annealing of structural defects caused by over 40 years of radiation damage, with no change in the fcc $Fm\bar{3}m$ crystal structure. Heating chloride-contaminated PuO_2 powder to ~230 °C and cooling back to ambient temperature in a sealed vessel reveals the production of H_2, He, NO and CO gases. More gas is produced from the untreated PuO_2 powder than PuO_2 which had previously been heat treated at 700 °C and the water adsorption/desorption behaviour of the two powders is remarkably different. The water sorption experiments described here are in agreement with theoretical calculations in the literature. The results from this study support the design of a heat treatment process to stabilise chloride-contaminated PuO_2, ready for long term storage.

Keywords

- Plutonium dioxide
- Chloride/water co-adsorption
- Thermal treatment
- Chemisorption/physisorption
- Stabilisation

1. Introduction

Plutonium dioxide (PuO_2), produced from the reprocessing of spent nuclear fuel, has been safely and securely stored in the UK for over fifty years, awaiting either reuse in mixed oxide (MOX) fuel or disposal in a geological disposal facility (GDF) [1–6]. Processing and storage of this material takes place at the Sellafield nuclear fuel reprocessing and decommissioning site in Cumbria, but a small fraction of the inventory has become contaminated with chloride. These legacy materials, dating mainly from the early 1970s, were stored in nested stainless steel containers with a polyvinyl chloride (PVC) intermediate layer. The chloride contamination is due to thermal and radiolytic degradation of the PVC bags, forming $HCl_{(g)}$, which has been adsorbed onto the surface of the

plutonium powder, together with water adsorbed from the air atmosphere in these non-welded ('breathable') packages. This chloride- and water-contaminated PuO_2 will require heat treatment in order to meet the conditions for acceptance (CFA) for repackaging and long term storage in modern facilities with welded cans. To underpin the design of the heat treatment process, it is necessary to characterise the chloride-contaminated powders and understand the process parameters which affect the partitioning of chloride between the product powder and off gas streams. The properties of the product (heat treated) powder, with respect to chloride species, also need to be determined, in order to establish its suitability for long term storage and the ultimate disposition options. Based on previous simulant PuO_2 experiments, chloride can be viewed as occurring in three different forms: volatilisable, which desorbs during heat treatment of the powder; leachable, which desorbs when the powder is washed with NaOH solution; and non-leachable, which remains either on the surface or within the powder when the powder is washed with NaOH solution. The heat treatment will volatilise some of the chloride, but evidence from simulant studies using PuO_2 artifically contaminated with chloride suggests that some of the chloride is very strongly bound to the PuO_2 [7].

CeO_2 is frequently used as a non-radiotoxic analogue to PuO_2, as it has the same fcc $Fm\overline{3}m$ crystal structure, +4 oxidation state and similar metal ion radius (Ce^{4+} = 0.97 Å and Pu^{4+} = 0.96 Å for 8 co-ordinate structures) [8][9][10]. Initial studies of Cl^- and water behaviour on CeO_2 have been carried out [11] and these experiments proved that:

i. chloride is not incorporated into the CeO_2 crystal structure, as no crystalline phases other than the fcc $Fm\overline{3}m$ phase of CeO_2 are present, but chloride does cause the average crystal size to increase by an as yet unidentified mechanism,
ii. the sorption mechanisms of water and chloride are linked and
iii. heat treatment at 900 °C removes chloride from the surfaces and the pores of high and low specific surface area CeO_2 particles (58 and 2 $m^2\ g^{-1}$, respectively).

The CeO_2 studies were then extended to cover the interactions of chloride and water with PuO_2, using samples of high purity PuO_2 ('Magnox PuO_2') obtained from the reprocessing of spent Magnox fuel (U metal fuel inside magnesium oxide cladding, which has produced UO_2, PuO_2, minor actinides and other fission products in a reactor) which were artificially contaminated with chloride and humidified in the laboratory [7]. Complementary sets of heat treatment experiments in a range of experimental conditions were utilised. The aims were to establish the likely behaviour of chloride-contaminated PuO_2 in heat treatment, changes in properties before and after heat treatment, and to determine any similarities between the PuO_2 and CeO_2 analogues. This work showed that no crystal phase change is observed between chloride-contamination, humidification and heat treatment of the PuO_2 samples. Self-irradiation damage, caused by α-decay, is annealed at high heat treatment temperatures. The PuO_2 crystals sinter at temperatures higher than the original calcination temperature. A fraction of the chloride adsorbed onto the PuO_2 surface is stable with respect to heat treatment, but is leachable with caustic solution at ambient temperature. We conclude that variations in PuO_2 specific surface area and production/storage history result in differences in behaviour, with respect to chloride desorption. These differences are likely to be accentuated by the different chloride sources used (dry HCl vapour versus PVC degradation) and environmental effects, including ageing. Thus, the behaviour observed with simulants may not be fully representative of the stored high chloride materials. The experiments also allowed a comparison of the results obtained

with PuO_2 and with CeO_2, where variations are expected, due to differences in redox properties, as Pu has a small gap between the 5f and 6d orbitals, whereas Ce has a larger gap between the 4f and 5d orbitals, which will be reflected in the electronic structure of the solid dioxides [12].

This paper reports the first studies on legacy chloride-contaminated PuO_2 powder retrieved from Sellafield stores, aiming to establish the likely inter-linked adsorption and desorption behaviours of chloride and water and their stabilities over a broad temperature range of relevance to the development of the heat treatment process. High temperature furnace experiments were carried out to study chloride-sorption, and lower temperature pressure vessel experiments were carried out to study water-sorption.

2. Experimental

2.1 PuO_2 – chloride interactions

Plutonium is an α-emitter, which presents both radioactivity and toxicity hazards. Manipulation and handling of these materials were performed only by qualified personnel in licensed radiological facilities.

The PuO_2 to be heat treated was poured into a borosilicate glass tube and inserted into a vertical tube furnace (1,000 °C INSTRON, UK) in an air atmosphere radiochemical (negative pressure) glove box. The airflow was set to 250 mL min^{-1} and the furnace was heated to the specified temperature at 10 °C min^{-1}, then held at temperature for 2 hours. The furnace was then left to cool with air flowing for 1 hour. The effluent gas was passed through an NaOH trap (25 mL, 0.5 mol L^{-1}). Once the apparatus had cooled, the trap was emptied and washed out with ultra high quality water (2 x 10 mL).

2.2 Determination of chloride

A subsample of the NaOH solution from the trap solution (4 mL) was analysed for chloride by ion chromatography (IC) before and after heat treatment. Subsamples of PuO_2 powder were also taken before and after heat treatment, added to 4 mL of fresh NaOH solution, shaken, left for a few days to separate and filtered for IC, using an Anotope inorganic alumina membrane filter (pore size = 0.2 µm and diameter = 10 mm). IC was performed using a Dionex DX-500 with an AS18 column and a mobile phase of NaOH (0.023 mol L^{-1}) (current = 76 mA, flow rate = 1.30 mL min^{-1} and conductivity stabilised at <5 µS). Standards of 2, 5, 7 and 10 ppm Cl^- were used. The samples were diluted in ultra high purity water by a factor of x100.

2.3 PuO_2 characterisation

For powder X-ray diffraction (XRD), the PuO_2 powders were immobilised in epoxy resin. The methods have been described previously [7]. The pucks were swabbed, then XRD patterns were recorded (Brücker D8) with step size = 0.02° and time per step = 9 s (2θ = 25-58°) and 18 s (2θ = 58-145°). Crystal sizes, lattice parameters and uncertainties were obtained from the XRD patterns using Topas software [13].

2.4 PuO_2 – water interactions

2.4.1 Sequential heating of Magnox PuO_2

Magnox PuO_2 was placed inside a custom-design pressurisable vessel (LBBC Baskerville, Leeds) (43.5 ± 1.2 cm^3), then heated in a Vecstar furnace inside an argon atmosphere glove box, which minimised nitrogen adsorption during loading, to an internal temperature of 100 °C at 5 °C min^{-1} and held at temperature for 4 hours. Keeping the vessel sealed, the `dry` heating/cooling cycle was repeated, but using peak furnace temperatures of 150, 200 and 230 °C. The 230 °C cycle was carried out twice. The head space gas in the vessel was sampled for gas chromatography (GC) with a Varian 490 micro GC with a 5Å molecular sieve column operating with an argon carrier gas. The vessel was opened and 0.05 mL water was added to a side chamber within the vessel, allowing the heating cycles to be repeated 'wet' with peak temperatures of 150 and 230 °C. This was done to understand the difference in PuO_2 behaviour and gas production when additional water is present in the vessel.

Baselines were recorded with the vessel open and subtracted from the recorded pressures, basing the second virial coefficient of water on the work of Harvey and Lemmon [14].

2.4.2 Magnox PuO_2 heat treated at 700 °C

Magnox PuO_2, previously heat treated at 700 °C, was placed in the pressure vessel. The vessel was placed in a furnace, then heated to an internal temperature of 225 °C (measured by two thermocouples within the vessel) at 5 °C min^{-1} and held at temperature for 4 hours. The furnace was left to cool and the pressure inside the sealed vessel was recorded throughout, using a pressure transducer. Without opening the vessel, the 'dry' heating and cooling cycle was repeated. After the second cycle the vessel was opened and 0.05 mL water was added to the side chamber, before being sealed and the two 'wet' heating cycles conducted to understand the difference in behaviour when additional water is present in the vessel.

3. Results

3.1 PuO_2 – chloride interactions

3.1.1 Ion Chromatography

An average of 2.9 monolayers of leachable chloride are present on the 0.5 and 1 g samples of untreated, contaminated PuO_2 before heat treatment (calculated using Eq. 1):

$$ML = \frac{mol_{adsorbed}}{n_m} \quad \textbf{(1)}$$

where $mol_{adsorbed}$ = number of moles of chloride adsorbed to the PuO_2 and n_m = number of moles of chloride per monolayer (1 monolayer of chloride is assumed to be 0.22 mg m^{-2}, the same as a water molecule) [15]. The uncertainties (± 9.3%) in the IC results shown are due to heterogeneity in the powder.

The amount of volatilised chloride present in the caustic trap after heating *c.f.* before heating is calculated using Eq. 2, and shown in Fig. 1.

$$Volatilised\ leachable\ chloride\ (\%) = \frac{(FC - SC)}{SS} * 100\% \quad \textbf{(2)}$$

The mass of chloride in the caustic trap after heat treatment is the final caustic (FC) and the mass of chloride in the caustic trap before heat treatment is the starting caustic (SC). The mass of leachable

chloride on PuO_2 before heat treatment is the starting solid (SS). The amount of chloride volatilised increases with heat treatment temperature. There is no difference in the percentage of chloride volatilised from either the 0.5 or 1 g samples of PuO_2. 100% represents the chloride which is leachable on the untreated solid; that is, the measurement from the leached solid made before heat treatment. More chloride than just the leachable component on the PuO_2 is volatilised at temperatures above 700 °C; i.e. the volatilised chloride measured is more than 100% of the initial leachable chloride, reflecting release of additional chloride from the non-leachable component.

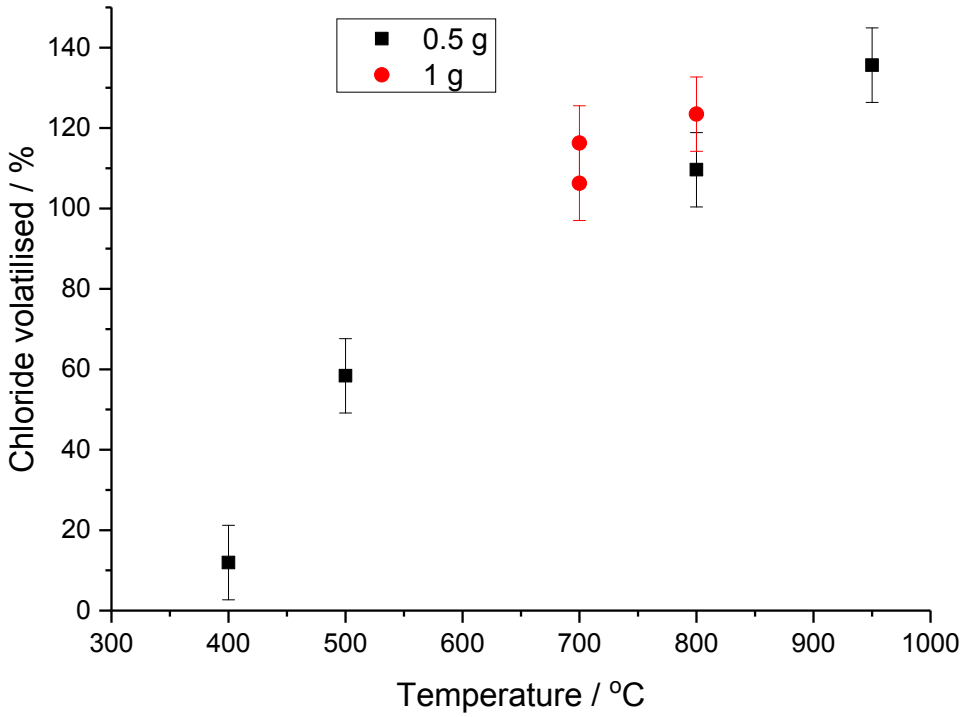

Figure 1: The percentage of chloride volatilised and trapped in the NaOH solution post-heat treatment, *c.f.* the leachable chloride on the solid PuO_2 pre-heat treatment.

Fig. 2 shows the average chloride concentration for the volatilised, leachable and non-leachable, which volatilises during treatment, fractions with heat treatment temperature for the 0.5 g and 1 g PuO_2 samples. All values are calculated relative to leachable chloride before heat treatment, which is taken as 100%. The difference in the chloride recovery between the initial analysis and the sum of the final leachable and volatilised chloride concentrations gives the 'non-leachable' component, calculated from Eq. 3:

$$Non-leachable\ fraction\ (\%) = \frac{(SS + SC) - (FS + FC) * 100\%}{SS} \quad \textbf{(3)}$$

The leachable chloride concentration on the PuO_2 solid after heat treatment is the final solid (FS). Fig. 2 shows that the leachable and non-leachable fractions on the solid decrease and the volatilised fraction increases with increasing heat treatment temperature. More chloride was recovered at

higher heat treatment temperatures in the 0.5 and 1 g PuO_2 starting material than when the powders were heated to low temperatures.

The leachable chloride remaining decreases quickly up to 700°C and then more slowly up to 950°C, reaching <2% at 800°C and 0% at 950°C for low mass starting material (0.5 and 1 g).

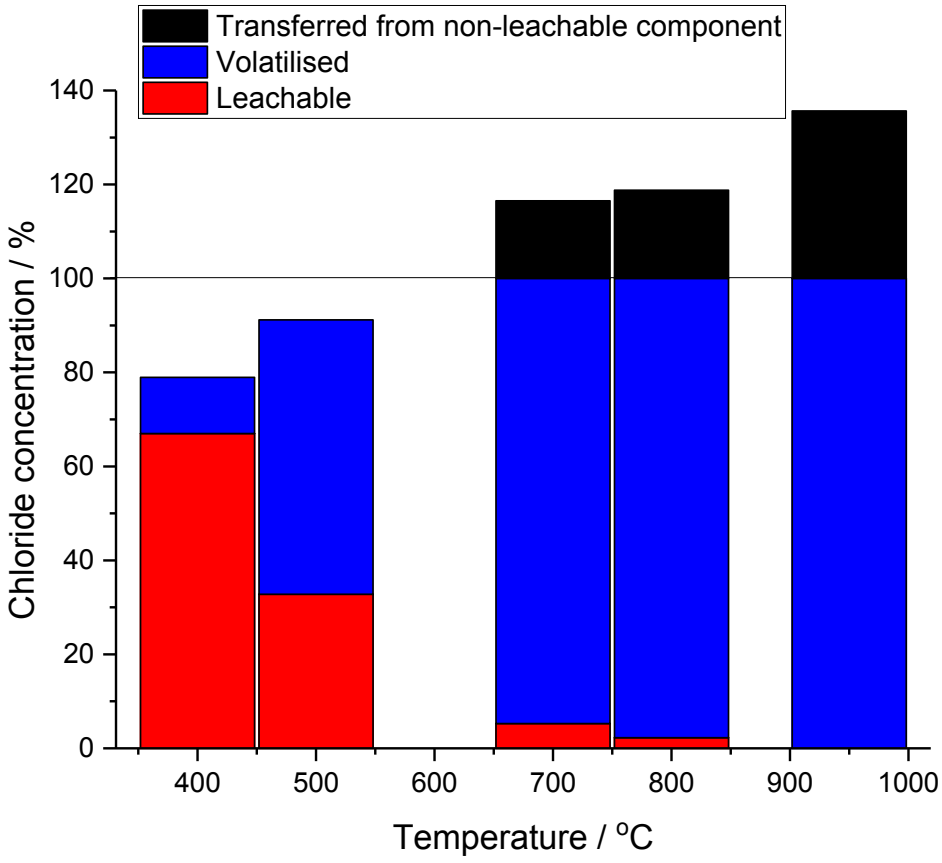

Figure 2: The percentage of chloride present in each of the leachable and volatilised fractions and the chloride transferred from the non-leachable to volatilised fractions, following heat treatment at a range of temperatures from the 0.5 g PuO_2 starting material samples, assuming 100% is leachable from untreated PuO_2.

3.1.2 X-Ray Diffraction

Powder XRD patterns of contaminated PuO_2 before and after heat treatment at 400, 600, 800 and 950°C are shown in Fig. 3. No additional phases are present in either the untreated or heat treated samples. The crystal sizes (calculated from the peak widths, using the Scherrer equation) increase with increasing heat treatment temperature, almost doubling in size following treatment at 950 °C (Fig. 4). The Bragg peak positions shift for each heat treatment temperature, indicating that the lattice parameters decrease with increasing temperature.

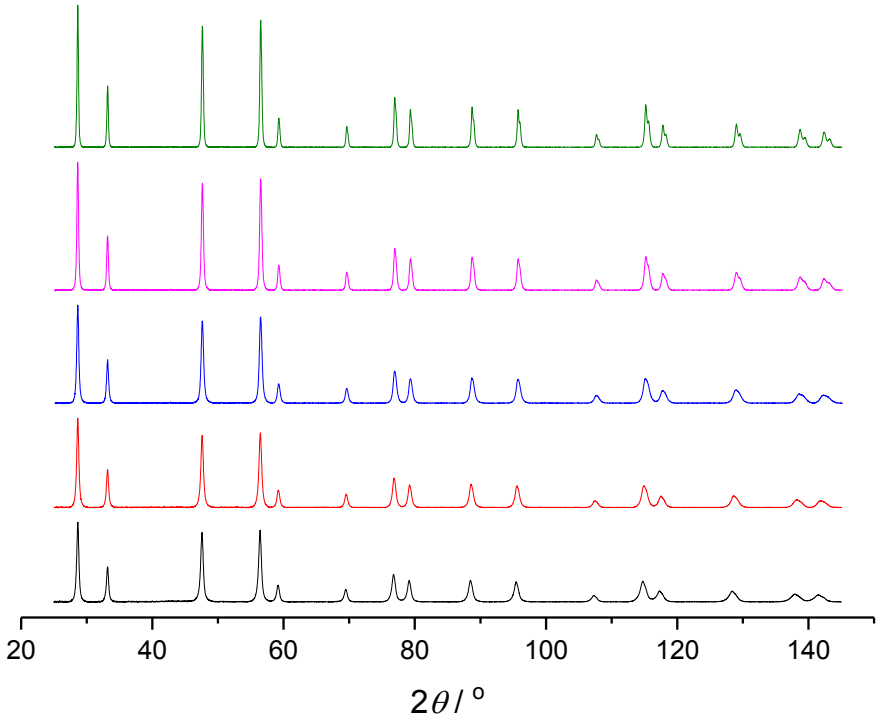

Figure 3: Powder XRD patterns of the contaminated Magnox PuO_2 untreated (black) and heat treated at 400 (red), 600 (blue), 800 (pink) and 950 °C (green).

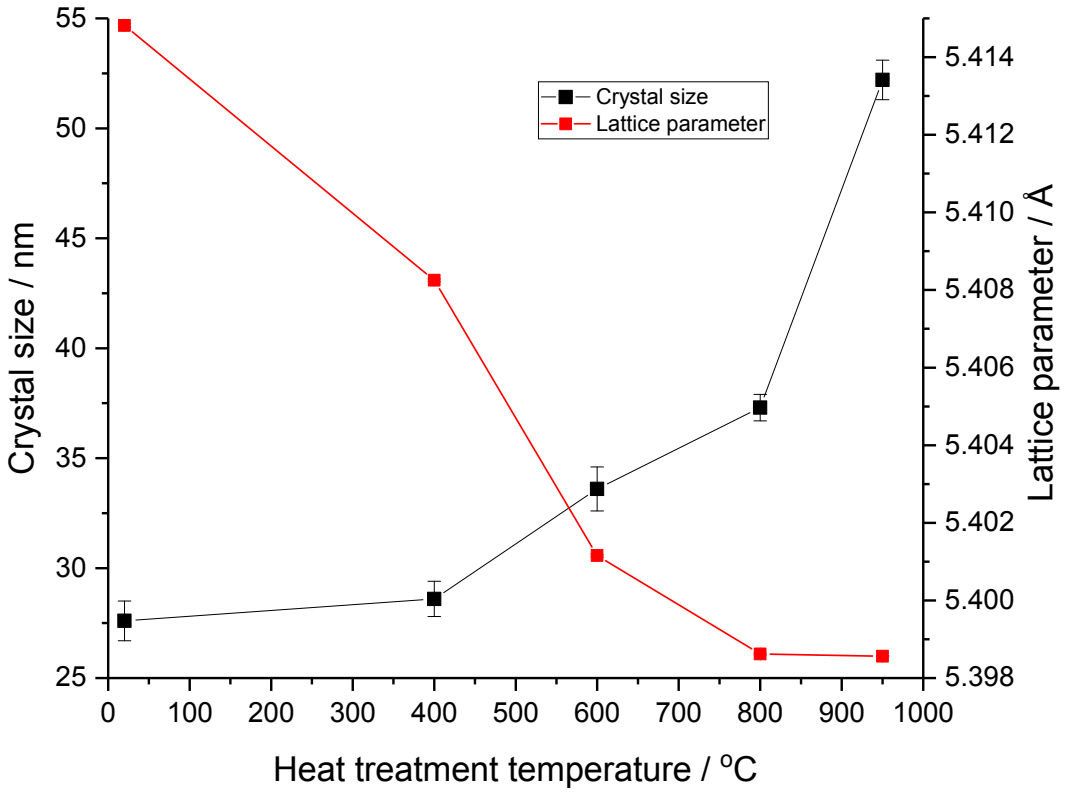

Figure 4: Crystal sizes and lattice parameters obtained from the XRD patterns in Fig. 3.

3.2 PuO_2 – water interactions

3.2.1 Sequential heating of Magnox PuO_2

The pressure variation with temperature for untreated, chloride-contaminated Magnox PuO_2 is shown (Fig. SI1). In the dry experiment, a gas is produced with each heating/cooling cycle and the linearity above ~113 °C indicates that the gas is ideal above this temperature. The final pressure increases after each cycle (± 10 Pa), compared to the starting pressure, even after heating the powder to 230 °C a second time (maximum permitted temperature in the Baskerville vessel). The total pressure increase due to the non-condensable gas produced at ambient temperature over the five cycles is 0.056 MPa. The gas produced is a mixture of He, H_2, O_2, N_2, NO and CO (Fig. SI2). The monolayers of water adsorbed to the surface of the PuO_2, calculated from the results obtained in Fig. SI1 during each heating/cooling cycle, are compared with the results obtained by Paffett *et al.* [15] in Figs. 5 and SI3, with relative humidity (RH) calculated using Eq. 4:

$$RH = \frac{P}{P_{SV}} \quad \textbf{(4)}$$

where P = pressure exerted by H_2O in the vessel (MPa) and P_{SV} = saturated vapour pressure at internal temperature $T_{internal}$ (MPa). The maximum number of monolayers able to physisorb to the PuO_2 surface, based on the sum of the measured water content of the PuO_2 and available moles of water added to the vessel, is shown, along with the number of strongly adsorbed monolayers (a

mixture of chemisorbed hydroxyls and molecular water and strongly physisorbed molecular water, defined by Haschke and Ricketts [16]), calculated as the intercept of the curve at 0% RH; the monolayers above this number are more weakly adsorbed and evaporate at these low temperatures.

In the wet experiments, the gas produced at temperatures >113 °C is non-ideal (Fig. SI4) and only a small amount is non-condensable (pressure increase inside the vessel = 0.021 MPa). The results from Fig. SI4 were used to calculate the monolayers of water adsorbed to the PuO_2 surface during each heating/cooling cycle (Fig. 6) and compared with the results of Paffett *et al*. [15]. The cumulative pressure increase within the Baskerville vessel at each maximum temperature is shown (Table 1); with each increasing maximum temperature in the Baskerville vessel, more gas is produced. The monolayers of water which are strongly adsorbed to the PuO_2 are calculated by extrapolating the experimental monolayer coverages to 0% RH (Table 2). The final pressure increase after each heating/cooling cycle and cumulative pressure increase since the start of the first cycle, *vs* the maximum temperature inside the vessel for the dry and wet sequential heating experiments are shown in Fig. 7.

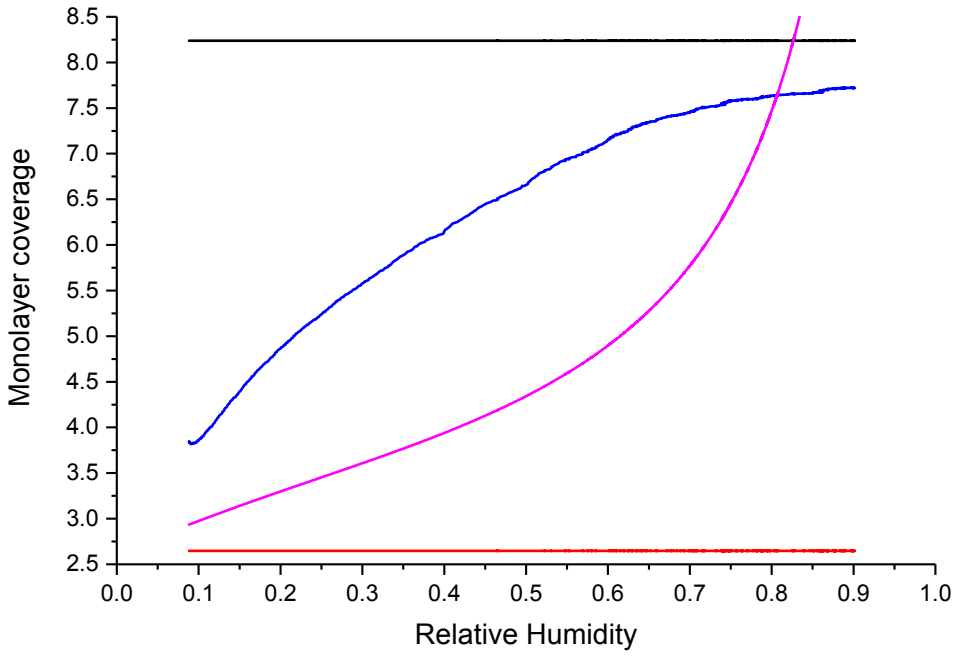

Figure 5: The calculated monolayers of water adsorbed to the PuO_2 obtained from the dry sequential heating Baskerville experiments (Fig. SI2) (blue) during the second cycle at 230 °C, plotted with the results obtained by Paffett *et al*. [15] (pink), the calculated strongly adsorbed monolayers of water (red) and the maximum number of water monolayers which can adsorb to the PuO_2 (black). The calculated monolayers for the cycles with peak temperatures = 100, 150, 200 and the first 230 °C are shown in Fig. SI3.

Table 1: The cumulative pressure increase after each cycle and variation of calculated relative humidity and monolayers of water remaining on the PuO_2 surface at the maximum temperature attained within the sealed vessel in the absence and presence of additional water, as derived from Figs. 5, 6 and SI3.

Maximum Temperature /	Cumulative Pressure	Relative Humidity	Water monolayers

°C	increase / MPa		
93.6 (dry)	0.00682	0.182	7.9
143 (dry)	0.01487	0.154	6.8
194 (dry)	0.03836	0.105	5.3
226 (dry)	0.04770	0.0930	4.0
225 (dry)	0.05596	0.0883	3.9
143 (wet)	0.00929	0.486	9.3
225 (wet)	0.02296	0.156	5.6

Table 2: The maximum temperature of each cycle and the monolayers of water strongly adsorbed at 0% RH, extrapolated from Figs. 5, 6 and SI3, using a polynomial gradient.

Maximum Temperature / °C	Water monolayers
93.6 (dry)	7.3
143 (dry)	5.2
194 (dry)	3.4
226 (dry)	2.4
225 (dry)	2.6
143 (wet)	7.3
225 (wet)	4.3

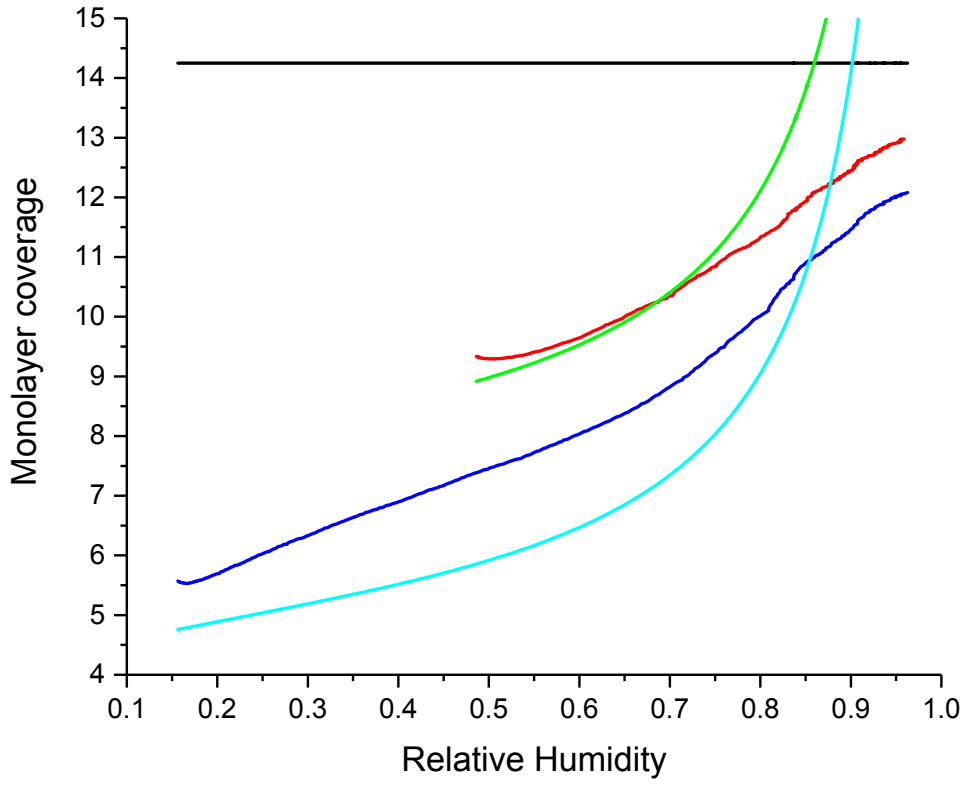

Figure 6: The calculated monolayers of water adsorbed to the PuO_2 obtained from the wet sequential heating Baskerville experiments (Fig. SI4) during the cycles at 150 °C (red) and 230 °C (navy), plotted with the results obtained by Paffett *et al.* [15] (150 °C = green and 230 °C = cyan) and the maximum number of water monolayers which can adsorb to the PuO_2 (black). The calculated strongly adsorbed monolayers of water for each cycle are shown in Table 2.

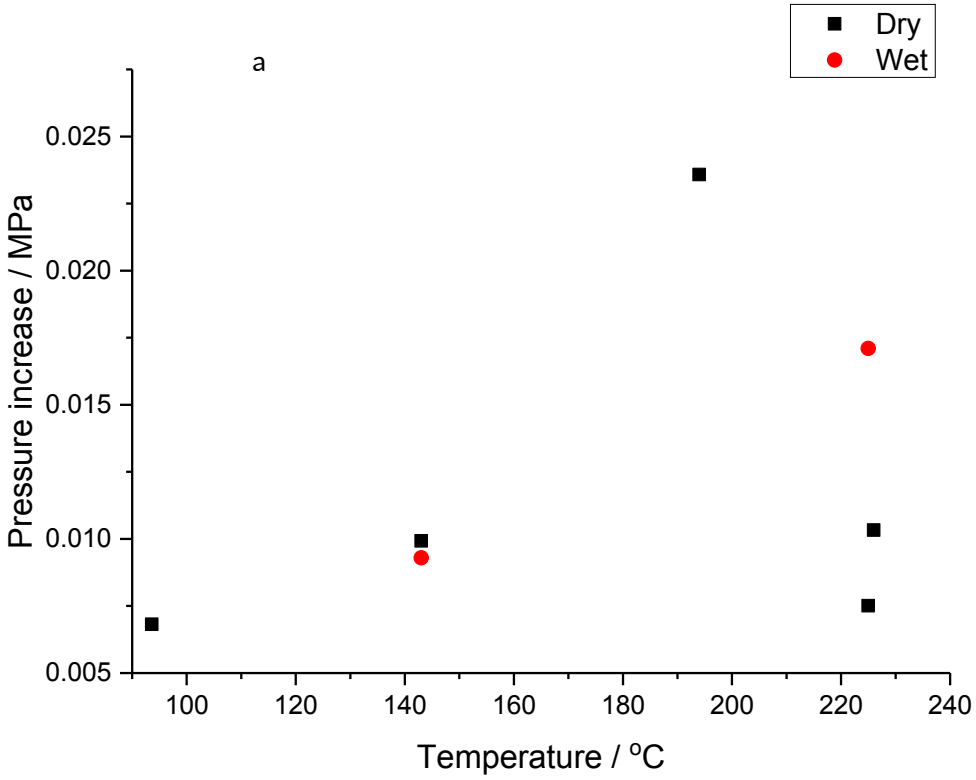
a
Dry
Wet
Pressure increase / MPa
0.025
0.020
0.015
0.010
0.005
100
120
140
160
180
200
220
240
Temperature / °C

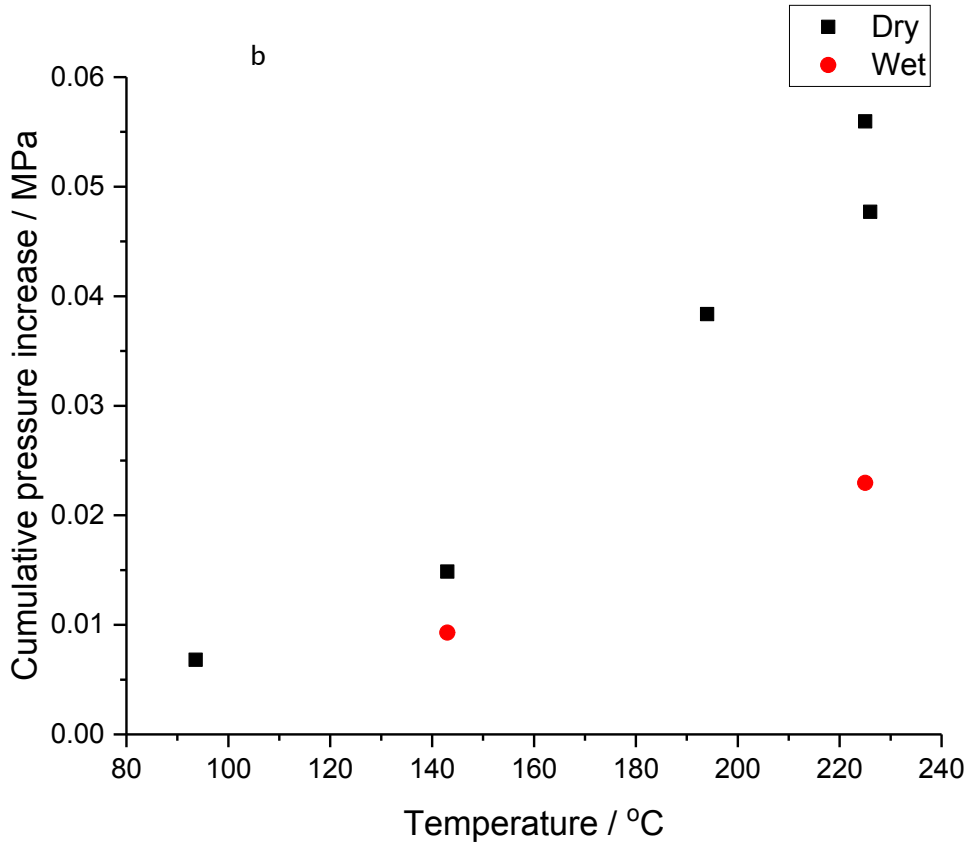
b
Dry
Wet
Cumulative pressure increase / MPa
0.06
0.05
0.04
0.03
0.02
0.01
0.00
80
100
120
140
160
180
200
220
240
Temperature / °C

Figure 7: Final pressure increase within the sealed vessel (a) following each heating/cooling cycle, relative to initial pressure before each cycle and (b) accumulated since the start of the first cycle *vs.* maximum temperature of the cycle for the dry and wet experiments, obtained from Table 1.

3.2.2 Magnox PuO_2 heat treated at 700 °C

Based on the above observation of a non-condensable gas, a second study was initiated using a sample of PuO_2 which had previously been heat treated at 700 °C. A sample was selected, which was considered to be broadly representative of a heat treated high chloride powder in order to assess its capacity for retaining and re-adsorbing water post-heat treatment. Fig. 8 shows the variation of pressure with temperature for the PuO_2. A `water only` cooling line (blue) is also displayed, calculated using the N_2 and saturated vapour pressures [14]. The first heating/cooling cycle of the PuO_2 in the Baskerville vessel without water shows that the pressure has increased, on cooling to ambient temperature, indicating that an ideal (shown by the linear pressure-temperature relationship), non-condensable gas has been produced. The pressure returns to the same elevated point after the second heating cycle, with no additional non-condensable gas being produced, giving a total pressure increase of 0.009 MPa.

Repeating this experiment with the same PuO_2 in the presence of water produces a pressure rise, which is due to a non-ideal gas, condensable on cooling to ambient temperature in both cycles (Fig. 9). More gas is produced in the wet experiment (maximum pressure at 225 °C = 0.374 MPa) than the dry experiment (maximum pressure at 225 °C = 0.171 MPa). Fig. SI5 shows the inverse relationship between RH and temperature measured within the vessel for the two wet heating/cooling cycles. Fig. 10 shows an increase in the amount of water (expressed as coverage of monolayers) adsorbed to the PuO_2 surface with relative humidity, calculated from Fig. 9. The results of this experiment differ from the results of Paffett *et al*. [15], particularly above RH *ca*. 0.5.

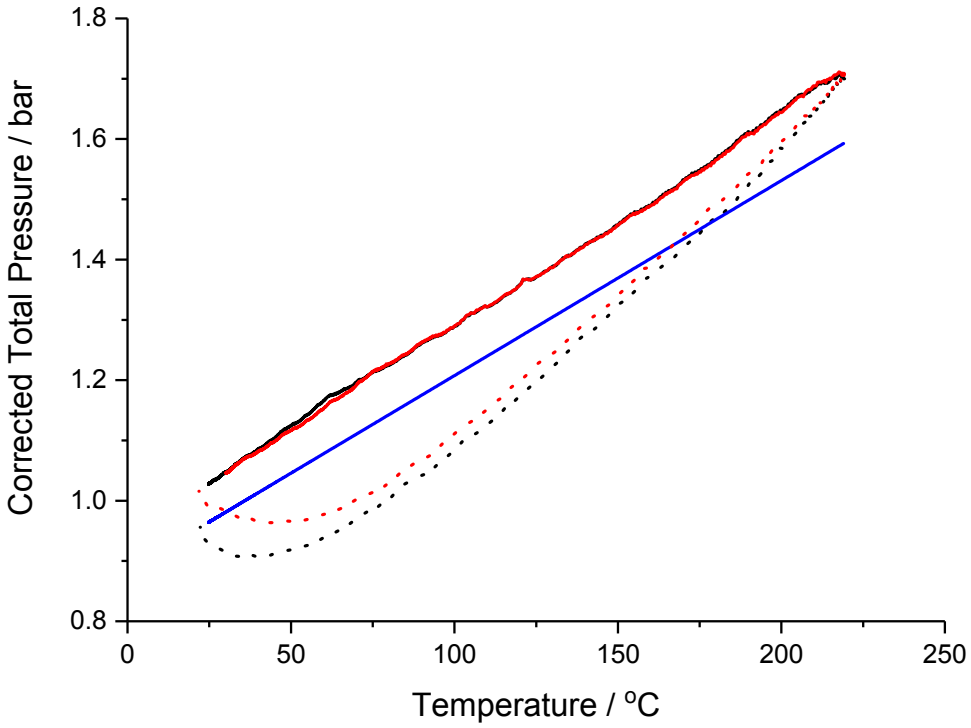

Figure 8: Variation of pressure with temperature for Magnox PuO_2, previously heat treated at 700 °C, inside the Baskerville vessel without water for two heating/cooling cycles (black = first and red = second, dotted line = heating and solid line = cooling); a calculated water only cooling line (blue) is also shown.

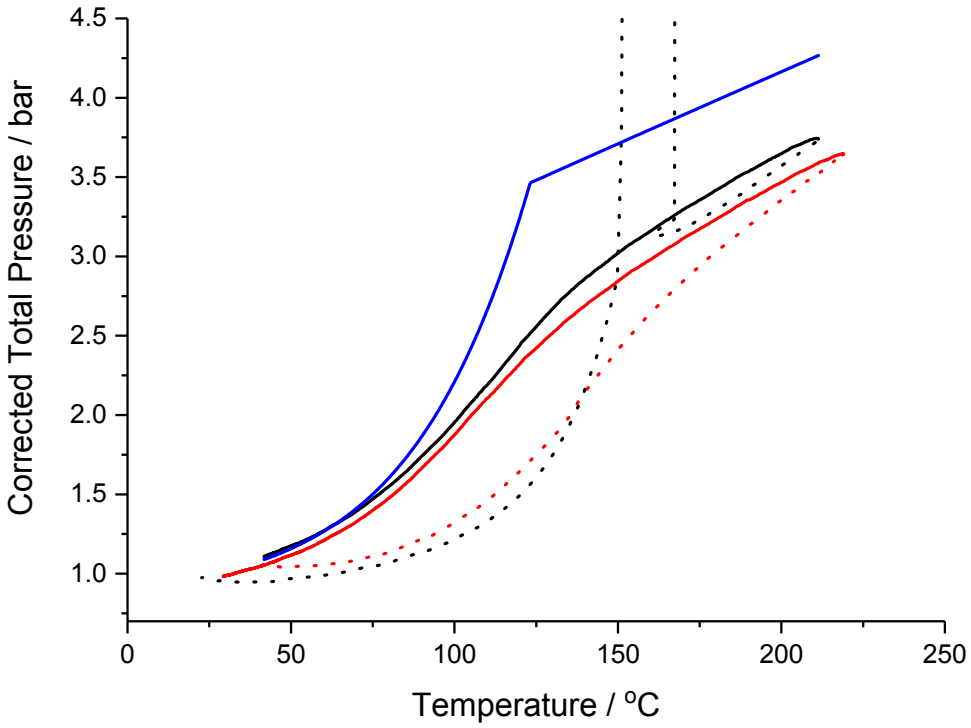

Figure 9: Variation of pressure with temperature for Magnox PuO_2, previously heat treated at 700 °C, inside the Baskerville vessel with 0.05 mL water in a side chamber over two heating/cooling cycles (black = first and red = second, dotted line = heating curve and solid line = cooling curve); a calculated water only cooling line (blue) is also shown. N.B. The sharp increase to an off-scale pressure on the first wet heating cycle (black) is due to a temporary fault in the pressure transducer; the furnace was switched off and once the pressure had returned to normal, heating was resumed and the experiment continued.

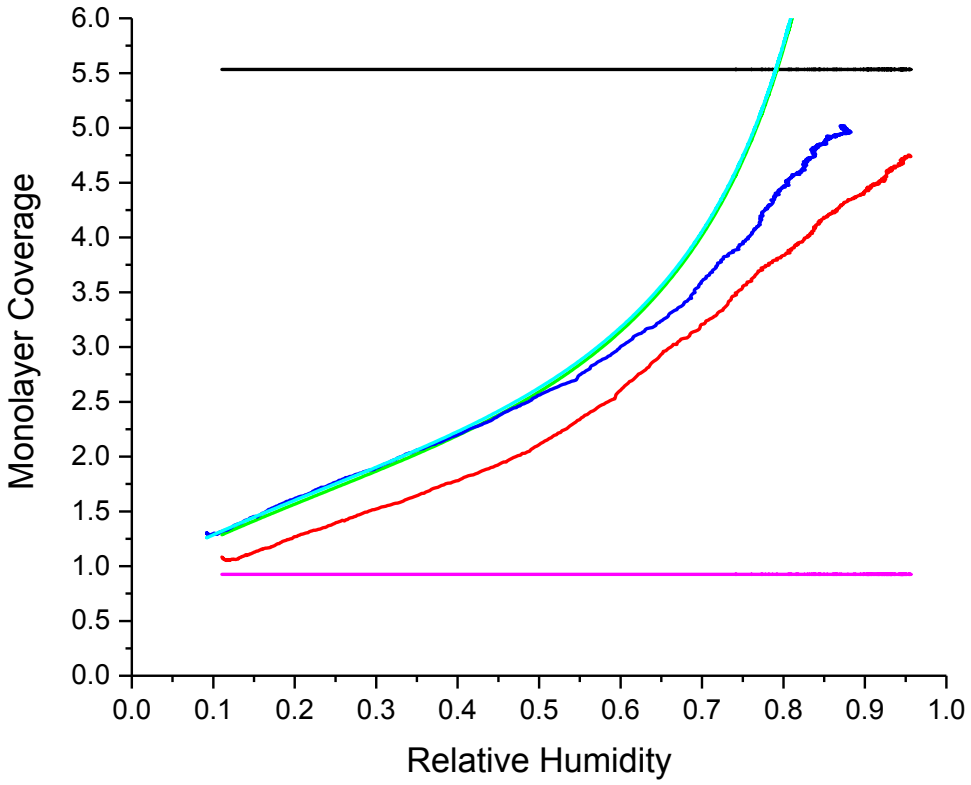

Figure 10: The variation of monolayer coverage of water on the PuO_2 surface with relative humidity, calculated from Fig. 9, showing the experimental results (cycle 1 = red and cycle 2 = navy), the results of Paffett et al. (cycle 1 = green and cycle 2 = cyan), the amount of strongly adsorbed water on the PuO_2 (pink) and the maximum amount of water which can be adsorbed to the PuO_2 (black) [15].

4. Discussion

4.1 PuO_2 – chloride interactions

4.1.1 Ion Chromatography

Identifying which species are present on the surface of the PuO_2 prior to heat treatment is beyond the scope of this study but, from the heat treatment data, it seems likely that there is a mixture of leachable and non-leachable species, based on previous studies by Parfitt *et al*. on TiO_2 surfaces and by the authors on artificially contaminated and humidified PuO_2 [7,17–21]. Since radiolytic degradation of plasticised PVC produces $HCl_{(g)}$ as the only chloride-containing contaminant, the presence of two forms of chloride on the PuO_2 surface highlights the complex chemistry of the PuO_2 surface [22–24]. The results show that when the PuO_2 powder is heat treated at <700 °C, less than 100% of the chloride leachable before heat treatment is recovered from the leachable and volatilised chloride after heat treatment. Even though some chloride is volatilised at these lower heat treatment temperatures, a significant proportion of leachable chloride remains bound to the PuO_2. However, more than 100% of the initial (leachable) chloride is detected in the caustic trap post-heat treatment at higher temperatures, with margins exceeding possible errors (*c.f.* pre-heat

treatment, Fig. 1). This suggests that there is a non-leachable chloride component either strongly bound on the surface or contained within the bulk PuO_2. It appears that heat treatment temperatures >700 °C can volatilise the non-leachable chloride species, by weakening the interactions between the PuO_2 and the adsorbed chloride as the specific surface area of the particles decreases. For example, in Fig. 2, IC of the leachable chloride remaining on the surface after heat treatment at 950 °C reduces to 0.0 ppm (± 1.4%), yet the percentage of chloride recovered from the caustic trap for this heat treatment temperature is 135% (*c.f.* the starting solid PuO_2).

Previous work on chloride-contaminated CeO_2 analogues revealed that the chloride homogeneously covered all available surface area, including within pores, but this was volatilised to the extent that the chloride remaining on the particles was below the limit of detection using energy dispersive X-ray analysis after heat treatment at 900 °C, showing that heat treatment removes chloride from all metal oxide surfaces, both exposed on the exterior of aggregates and within the aggregates [11]. The amounts of leachable chloride in the samples presented here are similar to those of simulant PuO_2, which was contaminated with dry HCl gas and humidified in the laboratory, before being heat treated at various temperatures [7]. However, the profiles for the simulant heat treated samples are significantly different and, overall, it appears that neither study generated wholly realistic simulants for the actual legacy chloride-contaminated PuO_2.

4.1.2 X-Ray Diffraction

The XRD pattern of the contaminated Magnox PuO_2 (Fig. 3) shows only the fcc $Fm\overline{3}m$ crystal phase and no phase change as the sample is heated. The crystal sizes of the untreated PuO_2 are 27.6 (± 0.9) nm (Fig. 4). This is similar to previous work carried out on simulant PuO_2, which was contaminated with dry HCl vapour and humidified and yielded a crystal size of 29.1 (± 0.8) nm. This crystal size is different to that of CeO_2 powders exposed to similar conditions, with CeO_2 powders calcined at 500 °C having crystal sizes of only 18.6 (± 1.5) nm, increasing to 46.1 (±11.3) nm when the powder was contaminated with dry HCl vapour [11]. The PuO_2 powders sinter and become more crystalline as the heat treatment temperature increases, especially above 600 °C, since the powders were originally calcined at 550 °C, as demonstrated by narrowing peak widths and increasing intensity, which was also seen for the nanocrystalline CeO_2 powders. The maximum crystal size for PuO_2 powders heat treated at 950 °C is 52.2 (± 0.9) nm.

The lattice parameters, calculated from the XRD patterns (Fig. 4), show that the lattice contracts as the heat treatment temperature increases, with the greatest difference in lattice parameters being between each of the low heat treatment temperatures, and only a small difference between the lattice parameters of the 800 and 950 °C samples. The lattice parameter for the 950 °C heat-treated PuO_2 powder sample (5.3986 Å) is larger than that reported by Farr et al. (5.3975 Å) for stoichiometric PuO_2 and by Chikalla et al. (5.3954 Å) for $^{238}PuO_2$; however, the sample heat treatment (950 °C) is not as effective as the temperatures used to anneal $^{238}PuO_2$ in these studies (>1,000 °C) [25,26]. The lattice has expanded over time, due to radiation damage from alpha decay of the Pu isotopes; heat treatment of the powders at higher temperatures anneals this damage and causes the lattice to contract [26–28]. The lattice parameter of the untreated, contaminated Magnox PuO_2 (5.4148 Å) is larger than that of simulant PuO_2, which has been contaminated with dry HCl vapour and humidified under laboratory conditions (5.4062 Å), as the Magnox PuO_2 studied here is

older, so has undergone more lattice damage [7]. Any defects caused by the contamination are also annealed, which is another possible cause of the volatilisation of non-leachable chloride.

4.2 PuO_2 – water interactions

4.2.1 Sequential heating of Magnox PuO_2

A small amount of helium is present in the gas sample, due to α-decay of the plutonium isotopes (Fig. SI2). Hydrogen from the radiolysis of adsorbed organics and water is produced in a significant quantity during the sealed vessel experiment. The production of H_2 from the radiolysis of adsorbed water to the PuO_2 surface is in agreement with theoretical studies [29,30] and experimental studies by Sims *et al*. and references therein [31]. The NO and CO species adsorbed to the PuO_2 surface are volatilised in this experiment, but are not oxidised, as these experiments were carried out in an argon atmosphere glove box. Only the cooling part of the cycle is considered henceforth, as hysteresis from rapid heating occurs and the thermocouples are in equilibrium with each other only during cooling. The maximum pressure reached at 230 °C is greater than that of the sample previously heat treated at 700 °C (0.505 MPa at 230 °C, *c.f*. 0.374 MPa at 225 °C). It is possible that even more gas (particularly helium from within the pores) would have evolved, had the 230 °C cycle been repeated more times or the peak temperature been higher.

Stakebake defines three types of water adsorption to the PuO_2 surface: (i) chemisorbed water, which forms strongly bound hydroxyls by dissociative adsorption onto Pu and O, (ii) quasi-chemisorbed molecular water, which either singly or doubly hydrogen bonds to the hydroxyls and (iii) physisorbed molecular water, which hydrogen bonds to adsorbed molecular water [32]. Haschke and Ricketts suggest that one monolayer of water tenaciously chemisorbs to the PuO_2 surface at low relative humidity and another monolayer physisorbs by RH of 0.50 [16]. The monolayers of water adsorbed to the PuO_2 (Figs. 5 and SI3 and Table 1) decrease with relative humidity as the peak temperature inside the Baskerville chamber increases, but the temperatures used here are not high enough to remove the strongly adsorbed water. Stakebake and Veirs *et al*. suggest that the chemisorbed hydroxyls cannot be desorbed below 1,000 °C and Farr *et al*. report the ubiquitous presence of surface hydroxyls when PuO_2 is exposed to water vapour, through both molecular and dissociative adsorption, which remain on the surface up to 590 °C [25,33]. Wellington *et al*. suggest that the first adsorbed water monolayer is either dissociatively or molecularly bound, depending on the Miller index of the surface [30]. Theoretical studies by Tegner *et al*. report the highest temperature of desorption of the hydroxylated PuO_2 (1 0 0) surface to be 377 °C under a pressure of 5 bar, higher than the maximum temperature the powder was heated to in these experiments of 226 °C [29]. The differences between the results of this study and previous theoretical data may have several causes, most notably the lack of chloride in the computational studies. As the Baskerville chamber cools to ambient temperature and the relative humidity increases, the desorbed water, which was condensed and weakly physisorbed on the PuO_2, as proposed by Haschke and Ricketts, re-condenses on the surface, so that ~8 monolayers are adsorbed after each cycle, close to the total amount of water measured on the PuO_2 before the experiment [16]. Haschke and Ricketts also proposed that up to 10 monolayers of water adsorb to PuO_2 at ambient temperature and RH of 1. The final pressure increase caused by non-condensable species peaks after the 200 °C cycle (Table 1 and Fig. 7a) and decreases after each of the 230 °C cycles, suggesting that the majority of the species volatilisable at this temperature have undergone sublimation. None of the species detected by gas

chromatography are of sufficient concentration to explain the pressurisation observed in this experiment. Therefore the dominant species produced by heating the PuO_2 must be a species such as CO_2, N_2O or Cl_2, which cannot be separated on the molecular sieve column.

When 0.05 mL water is added to the side chamber in the vessel, the gas produced when the Magnox PuO_2 powder is heated to 150 and 230 °C is completely non-ideal, even at temperatures >113 °C (Fig. 7). 13 monolayers of water are adsorbed to the PuO_2, following the wet cycle with peak temperature = 150 °C, and 12 after the wet cycle with peak temperature = 230 °C, once ambient temperature is reached (highest relative humidity) (Fig. 6), *c.f.* ~8 after each dry cycle (Figs. 5 and SI3), yet for the experiments carried out in this study, the maximum allowed monolayers are not exceeded (see section 3.2.1). Therefore, adding 0.05 mL water to the side chamber leads to 5 additional monolayers of water being adsorbed following the wet cycle at 150 °C; this is also observed following the wet cycles of the Magnox PuO_2 heat treated at 700 °C (see section 4.2.2), assuming no water was adsorbed following the dry cycles [17]. After the wet cycle at 230 °C, however, only 4 additional monolayers are readsorbed, *c.f.* the final pressure of the dry cycles. It is possible that the high chloride-contamination changes the water/chloride species on the PuO_2 surface, so that some water cannot readsorb once it has volatilised at these low temperatures. However, determining the chemical species present on the surface of the Magnox PuO_2 here requires further investigation by X-ray photoelectron spectroscopy (XPS) [25].

We propose that the high chloride content present on the untreated PuO_2 surface co-adsorbs additional water from the side chamber in the Baskerville vessel, giving rise to the large number of monolayers of water on the PuO_2. This is not observed in the 700 °C heat treated PuO_2 sample (see section 4.2.2), as most of the adsorbed chloride has been volatilised during heat treatment, so that less water is co-adsorbed using this mechanism upon condensation on the surface, and accounts for the difference in results *c.f.* Paffett *et al.* [15].

4.2.2 Magnox PuO_2 heat treated at 700 °C

During prior heat treatment at 700 °C under an air atmosphere, adsorbed volatile species, such as H_2O, CO_2 and NO_2, will have mostly been desorbed together with a substantial part of the chloride inventory [7]. However, after the PuO_2 sample was heat treated at 700 °C, it was stored in an air atmosphere glove box, potentially allowing oxidised gaseous species, such as H_2O, N_2 and CO_2, to re-adsorb to the PuO_2 surface (N_2 is subject to radiolysis and adsorption as NO_x) [7]. The gas released during the first Baskerville run, detectable on cooling the dry sample, is ideal and non-condensable at ambient temperature (Fig. 8). No more gas is evolved on heating the powder a second time. Noting that this is significantly less than the untreated sample, it is likely that this is due to desorption of the pre-adsorbed gases, particularly HCl.

Paffett *et al.* have reported that when this experiment is repeated with 0.05 mL water, during heating, a non-linear pressure increase with temperature indicates desorption of water until a plateau is reached, which is also observed in Fig. 9; this plateau and subsequent linear P-T relationship indicates the presence of an ideal gas [15]. The maximum pressure reached is less on the second cycle here than the first (0.364 *c.f.* 0.374 MPa respectively). This is the result of slow corrosion of PuO_2, producing a thickening hydroxide layer [15]. The gas produced is non-ideal, as it does not follow the modelled water only curve (blue line), and condenses on the liberated sites, based on the work done by Stakebake; thus, the final pressure after both wet heating/cooling cycles

returns to the initial pressure value at ambient temperature [32]. This also suggests that water is not the only gas in the vessel, after subtracting the baseline due to the glove box atmosphere. The adsorbed water from the first cycle has not completely volatilised by 225 °C, shown by the decreased relative humidity during the second cycle *c.f.* the first (Fig. SI5); some remains on the PuO_2 surface, where more water adsorbs on the second cycle, resulting in a higher number of adsorbed monolayers (Fig. 10) [34]. The monolayer coverage of water on the PuO_2 surface in this experiment (Fig. 10) does not decrease to less than the strongly adsorbed fraction (pink line) at low relative humidities in either the first or second cycle; thus, heating the PuO_2 powder to 225 °C removes water only in the weakly physisorbed fraction from the powder surface. The shape of the sorption curve and total (weakly and strongly) adsorbed water in this experiment are different to the untreated PuO_2 sample, but more similar to the observations of Paffett at low relative humidities, as the chloride has volatilised and the specific surface area has increased during heat treatment at 700 °C, so less co-adsorption of water occurs [15]. The experimental results also show that the monolayers of water adsorbed do not exceed the calculated maximum allowed (black line), even at high relative humidities. This differs from the results obtained by Paffett et al., where the monolayers exceed the maximum coverage at RH 0.79 and 0.80 (Fig. 10); the discrepancy between these results is possibly due to different surfaces being available in these experiments for the water to condense on, both on the equipment and the powder. The results presented here are in agreement with Haschke and Ricketts for the first wet cycle, but more water adsorbs to the PuO_2 in the second wet cycle [16].

5. Conclusions

The effects of heat treatment on chloride- and water-contaminated PuO_2 have been presented. As expected, high heat treatment temperatures of 700, 800 and 950 °C volatilise not only (almost) all of the leachable chloride present on the 0.5 g and 1 g PuO_2 starting material sample surfaces before heat treatment, but also some of the non-leachable fraction; however, furnace heat treatment at low temperatures changes the leachable chloride on the PuO_2 into a non-leachable fraction. Further studies are needed to investigate the chemistry of the non-leachable species and the amount present on the PuO_2. XRD of the PuO_2 powders shows that, similar to previous CeO_2 work, the high heat treatment temperatures sinter the nanocrystals and anneal the damaged PuO_2 lattice, leading to an increase in crystal size and a smaller lattice parameter. Water sorption experiments show that more non-condensable gas is produced when untreated Magnox PuO_2 is heated and cooled at progressively higher maximum temperatures (up to 230 °C) than pre-treated Magnox PuO_2, but this gas is only ideal above ~113 °C. When water is added to the side chamber, the gas produced is completely non-ideal and only partially condensable, as the presence of chloride on the untreated Magnox PuO_2 surface co-adsorbs more water than on the pre-treated Magnox PuO_2, where less chloride is present. Thermal cycling experiments on Magnox PuO_2, previously heat treated at 700 °C, have shown that an ideal, non-condensable gas is produced in the dry cycles. Untreated and pre-treated Magnox PuO_2 behave remarkably differently, with regards to water adsorption and the gases produced from the PuO_2 surface, and the presence of chloride on the untreated sample contributes to these differences. Even at very low relative humidity, there is at least one monolayer of water chemisorbed to the powder surface; at higher relative humidities, more water adsorbs, but only as weakly physisorbed water, which is in agreement with theoretical calculations on the presence of water on the PuO_2 surface. The temperatures used in the sealed vessel experiments are not high

enough to remove any strongly adsorbed water. Variations are expected between PuO_2 and CeO_2 studied previously, due to differences in redox chemistry for each compound, as Pu has a small energy level gap between the 5f and 6d orbitals, whereas Ce has a larger gap between the 4f and 5d orbital energy levels [12]. In order for repackaging of chloride- and water-contaminated PuO_2 to meet the conditions for acceptance, it must be heat treated at temperatures higher than 700 °C, in order to substantially remove chloride and water by volatilisation and anneal any defects caused by long term storage; however, water will re-adsorb to the PuO_2 surface upon cooling as RH increases, if the powder is subsequently exposed to an air atmosphere.

Acknowledgements

We thank the EPSRC and Sellafield Ltd. for a studentship (to SSH). All experiments were carried out with the aid of Kevin Webb, Colin Gregson, Stacey Reilly, Catherine Campbell, Hannah Colledge, Josh Holt and Bliss McLuckie at the National Nuclear Laboratory Central Laboratory, Sellafield, Cumbria, UK; access (for SSH) was funded by the Nuclear Decommissioning Authority. We also thank John Waters (University of Manchester) for his guidance with powder X-ray diffraction.

Data availability

The raw/processed data required to reproduce these findings cannot be shared at this time as the data also forms part of an ongoing study.

References

[1] L. Cadman, A. Goater, Managing the UK Plutonium Stockpile, 2016. researchbriefings.files.parliament.uk/documents/POST-PN-0531/POST-PN-0531.pdf.

[2] Nuclear Decommissioning Authority, Progress on approaches to the management of separated plutonium, 2014. doi:21100718.

[3] Department of Energy and Climate Change, Management of the UK's plutonium stocks: A consultation on the long-term management of UK owned separated civil plutonium, 2011.

[4] N.C. Hyatt, Plutonium management policy in the United Kingdom: The need for a dual track strategy, Energy Policy. 101 (2017) 303–309. doi:10.1016/j.enpol.2016.08.033.

[5] P. Cook, H. Sims, D. Woodhead, Safe and Secure Storage of Plutonium Dioxide in the United Kingdom, Actinide Research Quarterly. August (2013) 20–25.

[6] R. Taylor, J. Hobbs, R. Orr, H. Steele, Characterisation of plutonium dioxide, Nuclear Future. 14 (2018) 40–50.

[7] S. Sutherland-Harper, C. Pearce, C. Campbell, M. Carrott, H. Colledge, C. Gregson, J. Hobbs, F. Livens, N. Kaltsoyannis, R. Orr, M. Sarsfield, H. Sims, H. Steele, I. Vatter, L. Walton, K. Webb, R. Taylor, Characterisation and heat treatment of chloride contaminated and humidified PuO2 samples, Journal of Nuclear Materials. 509 (2018) 654–666. doi:10.1016/j.jnucmat.2018.07.031.

[8] H.S. Kim, C.Y. Joung, B.H. Lee, J.Y. Oh, Y.H. Koo, P. Heimgartner, Applicability of CeO2 as a surrogate for PuO2 in a MOX fuel development, Journal of Nuclear Materials. 378 (2008) 98–

104. doi:10.1016/j.jnucmat.2008.05.003.

[9] R.D. Shannon, Revised Effective Ionic Radii and Systematic Studies of Interatomic Distances in Halides and Chalcogenides, Acta Crystallographica Section A. 32 (1976) 751–767.

[10] M.C. Stennett, C.L. Corkhill, L.A. Marshall, N.C. Hyatt, Preparation, characterisation and dissolution of a CeO2 analogue for UO2 nuclear fuel, Journal of Nuclear Materials. 432 (2013) 182–188. doi:10.1016/j.jnucmat.2012.07.038.

[11] S. Sutherland-Harper, R. Taylor, J. Hobbs, S. Pimblott, R. Pattrick, M. Sarsfield, M. Denecke, F. Livens, N. Kaltsoyannis, B. Arey, L. Kovarik, M. Engelhard, J. Waters, C. Pearce, Surface speciation and interactions between adsorbed chloride and water on cerium dioxide, Journal of Solid State Chemistry. 262 (2018) 16–25. doi:10.1016/j.jssc.2018.02.018.

[12] J.C. Marra, Cerium as a surrogate in the Plutonium immobilization waste form, 2002.

[13] C.L. Corkhill, D.J. Bailey, F.Y. Tocino, M.C. Stennett, J.A. Miller, J.L. Provis, K.P. Travis, N.C. Hyatt, Role of Microstructure and Surface Defects on the Dissolution Kinetics of CeO2, a UO2 Fuel Analogue, ACS Applied Materials and Interfaces. 8 (2016) 10562–10571. doi:10.1021/acsami.5b11323.

[14] A.H. Harvey, E.W. Lemmon, Correlation for the Second Virial Coefficient of Water, Journal of Physical and Chemical Reference Data. 33 (2004) 369–376. doi:10.1063/1.1587731.

[15] M.T. Paffett, D. Kelly, S.A. Joyce, J. Morris, K. Veirs, A critical examination of the thermodynamics of water adsorption on actinide oxide surfaces, Journal of Nuclear Materials. 322 (2003) 45–56. doi:10.1016/S0022-3115(03)00315-5.

[16] J.M. Haschke, T.E. Ricketts, Adsorption of water on plutonium dioxide, Journal of Alloys and Compounds. 252 (1997) 148–156. doi:10.1016/S0925-8388(96)02627-8.

[17] G.D. Parfitt, J. Ramsbotham, C.H. Rochester, Infra-red study of hydrogen chloride adsorption on rutile surfaces, Transactions of the Faraday Society. 67 (1971) 3100. doi:10.1039/tf9716703100.

[18] P. Jackson, G.D. Parfitt, Infra-red study of the surface properties of rutile. Water and surface hydroxyl species, Transactions of the Faraday Society. 67 (1971) 2469. doi:10.1039/tf9716702469.

[19] J.W. Elam, C.E. Nelson, M.A. Tolbert, S.M. George, Adsorption and desorption of HCl on a single-crystal α-Al2O3(0001) surface, Surface Science. 450 (2000) 64–77. doi:10.1016/S0039-6028(99)01247-9.

[20] R. V Siriwardane, J.. Wightman, Interaction of hydrogen chloride and water with oxide surfaces, Journal of Colloid and Interface Science. 94 (1983) 502–513. doi:10.1016/0021-9797(83)90290-4.

[21] R.R. Bailey, J.P. Wightman, Interaction of gaseous hydrogen chloride and water with oxide surfaces, Journal of Colloid and Interface Science. 70 (1979) 112–123. doi:10.1016/0021-9797(79)90014-6.

[22] J. Colombani, V. Labed, C. Joussot-Dubien, A. Périchaud, J. Raffi, J. Kister, C. Rossi, High doses gamma radiolysis of PVC: Mechanisms of degradation, Nuclear Instruments and Methods in Physics Research, Section B: Beam Interactions with Materials and Atoms. 265 (2007) 238–244. doi:10.1016/j.nimb.2007.08.053.

[23] I. Boughattas, E. Pellizzi, M. Ferry, V. Dauvois, C. Lamouroux, A. Dannoux-Papin, E. Leoni, E. Balanzat, S. Esnouf, Thermal degradation of γ-irradiated PVC: II-Isothermal experiments, Polymer Degradation and Stability. 126 (2016) 209–218. doi:10.1016/j.polymdegradstab.2015.05.010.

[24] A.H. Zahran, E.A. Hegazy, F.M. Ezz Eldin, Radiation effects on poly (vinyl chloride)-I. gas evolution and physical properties of rigid PVC films, Radiation Physics and Chemistry. 26 (1985) 25–32. doi:10.1016/0146-5724(85)90028-7.

[25] J.D. Farr, R.K. Schulze, M.P. Neu, Surface chemistry of Pu oxides, Journal of Nuclear Materials. 328 (2004) 124–136. doi:10.1016/j.jnucmat.2004.04.001.

[26] T.D. Chikalla, R.P. Turcotte, Self-radiation damage ingrowth in 238 PuO 2, Radiation Effects. 19 (1973) 93–98. doi:10.1080/00337577308232225.

[27] N.P. Turcottes, T.D. Chikalla, Annealing of self-radiation damage in 238 PuO2, Radiation Effects. 19 (1973) 99–108. doi:10.1080/00337577308232226.

[28] W.J. Weber, Alpha-irradiation damage in CeO2 , UO2 and PuO2, Radiation Effects. 83 (1984) 145–156. doi:10.1080/00337578408215798.

[29] B.E. Tegner, M. Molinari, A. Kerridge, S.C. Parker, N. Kaltsoyannis, Water adsorption on AnO2{111}, {110}, and {100} surfaces (An = U and Pu): A density functional theory + U study, Journal of Physical Chemistry C. 121 (2017) 1675–1682. doi:10.1021/acs.jpcc.6b10986.

[30] J.P.W. Wellington, A. Kerridge, J. Austin, N. Kaltsoyannis, Electronic structure of bulk AnO2(An = U, Np, Pu) and water adsorption on the (111) and (110) surfaces of UO2and PuO2from hybrid density functional theory within the periodic electrostatic embedded cluster method, Journal of Nuclear Materials. 482 (2016) 124–134. doi:10.1016/j.jnucmat.2016.10.005.

[31] H.E. Sims, K.J. Webb, J. Brown, D. Morris, R.J. Taylor, Hydrogen yields from water on the surface of plutonium dioxide, Journal of Nuclear Materials. 437 (2013) 359–364. doi:10.1016/j.jnucmat.2013.02.040.

[32] J.L. Stakebake, A Thermal Desorption Study of the Surface Interactions between Water and Plutonium Dioxide, The Journal of Physical Chemistry. 77 (1973) 581–586. doi:10.1021/j100624a003.

[33] D.K. Veirs, M.A. Stroud, J.M. Berg, J.E. Narlesky, L.A. Worl, M.A. Martinez, A. Carillo, MIS High-purity plutonium oxide metal oxidation product TS707001 (SSR123): Final report, 2017.

[34] D. Wayne, Thermal and Physical Properties of Plutonium Dioxide Produced from the Oxidation of Metal: a Data Summary, 2014.

Supplementary Information

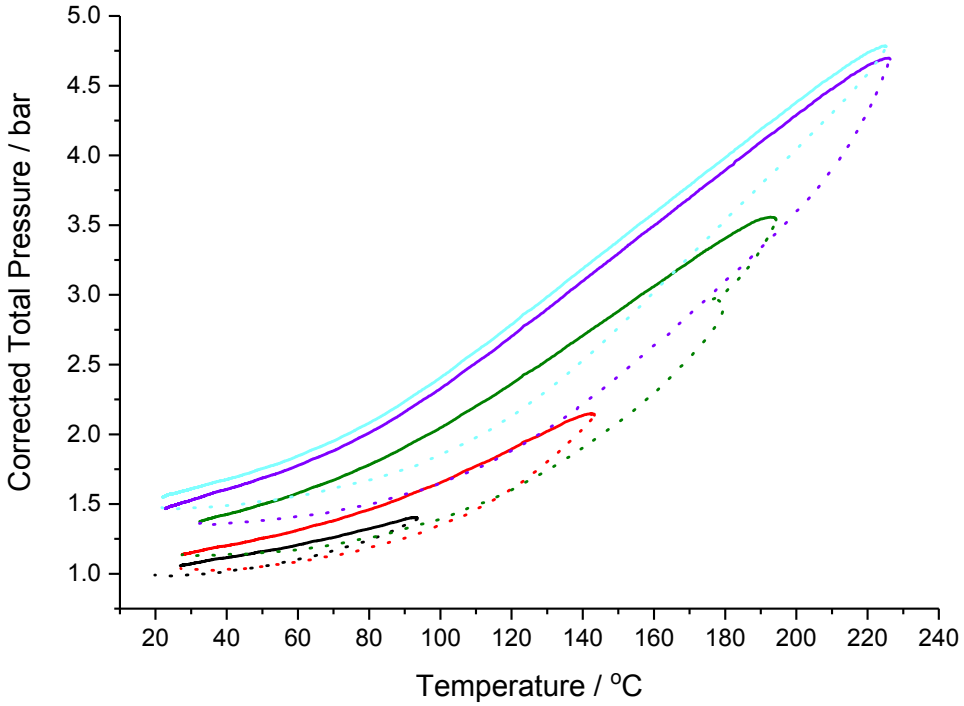

Figure SI1: Variation of pressure with temperature for contaminated Magnox PuO_2 inside the Baskerville vessel with maximum furnace temperatures of 100 (black), 150 (red), 200 (green) and 230 °C (two cycles, dark and light blue) without water (dotted line = heating curve and solid line = cooling curve).

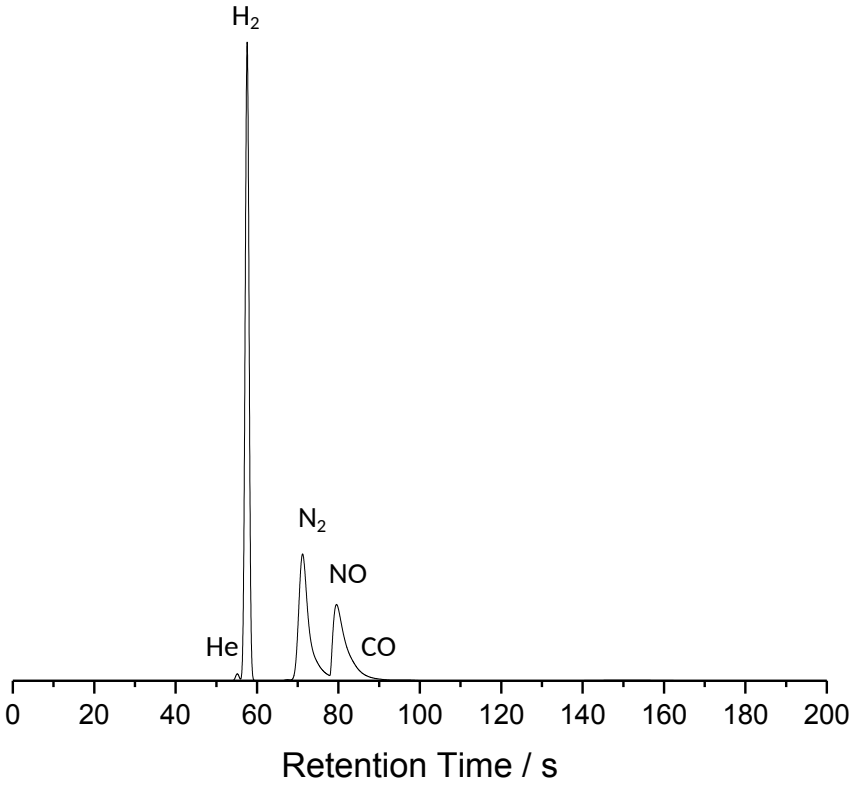

Figure SI2: Chromatogram of the gas sampled from the Baskerville vessel after heating/cooling cycles of dry chloride-contaminated PuO_2 (experiments illustrated in Fig. SI1). The N_2 detected is either due to contamination of the gas chromatography sample from air leaking into the glove box or contamination of the PuO_2 powder.